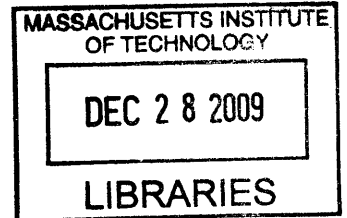


**Design and Development of High Precision Elastomeric-Stamp  
Wrapping System for Roll-to-Roll Multi-Layer Microcontact Printing**

by

Charudatta Achyut Datar

B.E. Mechanical Engineering  
University of Pune, 2007



Submitted To The Department Of Mechanical Engineering  
In Partial Fulfillment Of The Requirements For The Degree Of

Master of Engineering in Manufacturing

**ARCHIVES**

at the

MASSACHUSETTS INSTITUTE OF TECHNOLOGY

SEPTEMBER 2009

© 2009 Charudatta Achyut Datar.  
All rights reserved.

The author hereby grants to MIT permission to reproduce and to distribute publicly paper and electronic copies of this thesis document in whole or in part in any medium now known or hereafter created.

Signature of Author.....

A handwritten signature in black ink, appearing to read "Charudatta Achyut Datar".

Department of Mechanical Engineering  
18 August 2009

Certified by.....

A handwritten signature in black ink, appearing to read "David E. Hardt".

David E. Hardt  
Professor of Mechanical Engineering  
Thesis Supervisor

Accepted by.....

A handwritten signature in black ink, appearing to read "David E. Hardt".

David E. Hardt  
Chairman, Departmental Committee on Graduate Studies  
Department of Mechanical Engineering

# **Design and Development of High Precision Elastomeric-Stamp Wrapping System for Roll-to-Roll Multi-Layer Microcontact Printing**

by

Charudatta Datar

Submitted to the Department of Mechanical Engineering on 18 August, 2009,  
in partial fulfillment of the requirements for the  
Degree of Masters of Engineering in Manufacturing

Advisor: Dr. David E. Hardt

## **Abstract**

Microcontact printing is an emerging printing technique that could potentially find application in the electronics industry. High-speed roll-to-roll equipment was built at Nano Terra, Inc in 2008, for microcontact printing. However, the equipment was a proof-of-concept, capable of single-layer printing, while the industry requires a multi-layer printing capability. In addition, the quality of printing it delivered was not industry competitive. The existing equipment has thus been upgraded with a view to achieve high-precision multi-layer microcontact printing; including a new method to manufacture a flat stamp, design of a high-precision wrapping system, design of a five-axis positioning system, and modification of the impression roller. This thesis describes in detail the design of an innovative high-precision system to wrap the elastomeric stamp on the print roller. This is followed by results of multi-layer printing experiments, using the improved equipment. The potential for microcontact printing as a forthcoming technology for the electronics industry was confirmed. Further improvements are also suggested that would help deliver this promise.

## **Acknowledgements**

First and foremost, I would like to thank Professor David Hardt for his technical guidance and mentoring throughout this project.

My teammates, Paolo Baldesi, Wenzhuo Yang, and Yufei Zhu made this an enriching learning experience. In particular, it was a pleasure working alongside Paolo Baldesi for most part of the project.

At Nano Terra, Inc, I thank Shih-Chi Chen for sharing his wealth of knowledge and experience with the team, and for guiding us at every step of the project. I am also very grateful to Brian Mayers, and the entire staff at Nano Terra, Inc. for helping make this project a success.

I am especially grateful to Nevan Hanumara, my mentor at MIT, for his timely and valuable advice throughout the summer.

Finally, I thank my friends and family for their encouragement and support throughout.

## Table of Contents

<b>List of Tables .....</b>	<b>9</b>
<b>1 Introduction .....</b>	<b>10</b>
<b>1.1 Motivation.....</b>	<b>10</b>
<b>1.2 Problem Statement.....</b>	<b>11</b>
<b>1.3 Primary Analysis .....</b>	<b>12</b>
<b>1.4 Scope.....</b>	<b>13</b>
<b>1.5 Task Division .....</b>	<b>13</b>
<b>2 Literature Review.....</b>	<b>15</b>
<b>2.1 Soft Lithography.....</b>	<b>15</b>
<b>2.2 Micro-contact Printing.....</b>	<b>16</b>
<b>2.3 Existing Roll-to-Roll Equipment.....</b>	<b>18</b>
<b>2.4 Stamp Casting Machine.....</b>	<b>20</b>
<b>2.5 PDMS Peeling Process.....</b>	<b>22</b>
2.5.1 Stress Zones at PDMS Peel-Front.....	22
2.5.2 Initiating Peeling .....	23
<b>2.6 Multi-Layer Printing.....</b>	<b>24</b>
<b>2.7 Optical Methodology System Review.....</b>	<b>26</b>
2.7.1 Laser Triangulation Sensors .....	26
2.7.2 Interferometer Sensors .....	27
2.7.3 Fiber Optic Sensors .....	29
2.7.4 Con-Focal Laser Scanning Microscopy .....	31
<b>3 Methodology.....</b>	<b>33</b>
<b>3.1 Stamp Casting Machine.....</b>	<b>33</b>
<b>3.2 Peeling and Wrapping the Stamp on the Print Roller .....</b>	<b>35</b>
3.2.1 Gripping the Film for Peeling.....	35
3.2.2 Methods to Generate Adhesive Force Between Backing Plate and Print Roller	36
3.2.3 Methods to Wrap Backing Plate without Loosing Alignment.....	37
3.2.4 Analysis of Fixture System.....	38
<b>3.3 Precision Measurement Method .....</b>	<b>39</b>
3.3.1 Flatness and Roundness Measurement.....	39
3.3.2 Distortion Measurement.....	42
3.3.3 Measurement of the Accuracy of the Alignment .....	45
<b>4 The Wrapping Problem .....</b>	<b>46</b>
<b>4.1 Overall Goal .....</b>	<b>46</b>
<b>4.2 The Existing Wrapping Process.....</b>	<b>46</b>
<b>4.3 Requirements of Proposed Wrapping System: .....</b>	<b>48</b>
<b>4.4 The Peeling Process Design: .....</b>	<b>48</b>
<b>4.5 Design of Mechanics of First Contact .....</b>	<b>49</b>
4.5.1 Alignment Mechanism .....	49
4.5.2 Sources of Error during Alignment .....	49
4.5.3 Alignment Process .....	53
<b>5 Design .....</b>	<b>54</b>
<b>5.1 Wrapping System .....</b>	<b>54</b>

5.1.1	Concept Selection.....	54
5.1.2	Experiments to Simulate the Peeling-Wrapping Process:.....	55
5.1.3	Experiment #1: Simulation of the new peeling-wrapping process.....	55
5.1.4	Results: .....	56
5.1.5	Wrapping Demonstration with Sample Magnetic Cylinder and Backing Plate: .....	58
5.1.6	Design of Print Roller .....	59
5.1.7	Design of Backing Plate .....	61
<b>5.2</b>	<b>Mounting of the Print Roller onto the MIT '08 Machine.....</b>	<b>65</b>
5.2.1	Flexible Coupling Design.....	66
5.2.2	Design to Enable X-Axis Positioning.....	69
5.2.3	Shaft and Linear Rotary Bearings Design.....	71
5.2.4	Linear Rotary Bearing.....	71
5.2.5	Shaft Design.....	74
5.2.6	Thrust Bearing.....	75
<b>6</b>	<b>Results.....</b>	<b>76</b>
6.1	New Wrapping Process Results .....	76
6.2	Assumptions and Discussion:.....	79
<b>7</b>	<b>Flat Stamp Casting <sup>[24]</sup>.....</b>	<b>80</b>
7.1	Updated Flat Stamp Casting Machine .....	80
7.2	Wafer Chuck .....	80
7.3	Stainless Steel Vacuum Chucks .....	81
7.4	Assembly of Stamp Casting Machine.....	82
<b>8</b>	<b>Multi-layer Printing with Updated Roll-to-Roll System <sup>[34]</sup>.....</b>	<b>83</b>
8.1.1	Introduction of Multi-Layer Printing Process.....	83
<b>9</b>	<b>Conclusions and Future Work.....</b>	<b>86</b>
9.1	Conclusions.....	86
9.2	Future Work.....	87
<b>Appendix A Engineering Drawings, Wrapping System.....</b>		<b>89</b>
<b>Bill of Materials, Wrapping System .....</b>		<b>93</b>
<b>References .....</b>		<b>94</b>

## List of Figures

Figure 1: Illustration of The Self-Assembly Process <sup>[2]</sup> .....	16
Figure 2: Steps Involved in Micro-Contact Printing <sup>[3]</sup> .....	17
Figure 3: Concept of The Machine <sup>[4]</sup> .....	18
Figure 4: Layout of The Three Modules in The Equipment <sup>[4]</sup> .....	19
Figure 5: The R2R Machine Built in '08 [4] .....	19
Figure 6: Main Parts of Aluminum Casting Machine for Large Area Stamp, Developed by Nano-Terra LLC. ....	21
Figure 7: Illustration of Separation at The PDMS-Silicon Wafer Boundary <sup>[22]</sup> .....	23
Figure 8: Directions of Peeling Force <sup>[22]</sup> .....	23
Figure 9: Gravure Printing Machine. ....	24
Figure 10: Actuation Method For Adjusting The Relative Distance Between Print Nips on The Substrate. ....	25
Figure 11: Simplified Sensing Method For Detecting The Relative Position Between Two Layers of Print in Gravure Printing. ....	25
Figure 12: Principal of Laser Triangulation Sensor [14] .....	26
Figure 13: Principal of Interferometer System [15] .....	28
Figure 14: Total Internal Reflection inside Optical Fiber [15] .....	29
Figure 15: Fiber Optic Probe Configuration [17] .....	30
Figure 16: Fiber Optic Probe Response Curve [17] .....	30
Figure 17: Principal of Con-Focal Microscopy [23] .....	31
Figure 18: Structure for Wafer Chuck .....	33
Figure 19: Teflon Spacer .....	34
Figure 20: Sidebars Used to Align Both Chucks .....	34
Figure 21: Illustration of Pint Roller Setup before Wrapping .....	35
Figure 22: Illustration of The Proposed Fixture System .....	38

Figure 23: Fixtures for Flatness and Roundness Measurement .....	40
Figure 24: VERITAS VM 250 .....	40
Figure 25: Measurement Setting for Roundness Measurement .....	42
Figure 26: The Shape of Rectangular- like Pixel.....	43
Figure 27: The Shape of Triangular Pixel .....	43
Figure 28: The Array of Two Kinds of Pixels.....	43
Figure 29: Demonstration of the Distortion .....	44
Figure 30: Pixel Dimensions [20] .....	44
Figure 31: Displacement of Two Printed Layers .....	45
Figure 32: A section view of the existing stamp-roller interface [4].....	47
Figure 33: This figure shows a significant air gap between the print roller and the backing plate from the MIT '08 configuration .....	47
Figure 34: Shows calculation of error angle due to clearance between pins and holes .....	51
Figure 35: Gray: Ideal position of backing plate, Blue: Rotated position of backing plate due to clearance between holes and pins, Red: Angular Error .....	52
Figure 36: Illustration of setup before wrapping.....	53
Figure 37: Illustration of setup before wrapping.....	55
Figure 38: Shows the magnetic strips on the magnetic cylinder, and its conventional application in the die-cutting industry. The flexible plate being attached to the cylinder is patterned. [35] .....	57
Figure 39: The non-magnetic arc in the print roller .....	58
Figure 40: Illustration showing non-magnetic area on the print roller .....	59
Figure 41: Illustration of the print roller; Yellow: non-magnetic area for the peeling-wrapping process. Gray: Area not covered by backing plate, hence non-magnetic. Teal: Magnetic strips (not to scale) .....	60
Figure 42: Photo of Final Roll Provided by Rotometrics, showing the non magnetic part of sleeve.....	60
Figure 43: Determination of the position of alignment hole and slot in backing plate (illustration not to scale) .....	62

Figure 44: Derivation of strain elongation in beams subjected to pure moment bending. This is equivalent constant radius deformation as is the case here [33] .....	63
Figure 45: CAD model of the new print roller mounted on the Precision Positioning System [1] .....	65
Figure 46: Shows the chosen Flexible Coupling [39] .....	68
Figure 47: Rotary Linear Bearing [37] .....	71
Figure 48: Load Correction Factor [27].....	72
Figure 49: Load Factor [28].....	73
Figure 50: Thrust Bearing [36] .....	75
Figure 51: Illustrates backing plate wrapped on the magnetic sleeve. The red and the green frame show locations of photos used for analyzing wrapping precision .....	76
Figure 52: Shows an edge of the backing plate (red frame from Figure 51) .....	77
Figure 53: Shows an edge of the backing plate (green frame from Figure 51) .....	77
Figure 54: The enlarged photo shows the error, or misalignment during wrapping between the two edges of the backing plate. ....	78
Figure 55: Schematic illustration of the casting machine .....	80
Figure 56: 3D Model of Wafer Chuck for 12" wafer [24].....	81
Figure 57: 3D Model of Adapter of SS Chuck for 200mmx200mm Stamp Fabrication [24]. ...	81
Figure 58: 3D Model of Assembly for 12" wafer (exploded view). The wafer chuck is represented by a wireframe for a clearer view inside the structure. [24] .....	82
Figure 57: Position of Patterns After First Layer Printing [34].....	83
Figure 58: Alignment of the First Layer [34].....	84
Figure 59: Using Microscope to Align the Position of the Substrate [34].....	84
Figure 60: Adjustment of Second Layer printing [34].....	85



**List of Tables**

Table 2: Coupling Selection [32] ..... 67

Table 3: Pugh Chart..... 70

Table 4: Maximum Allowable Loads [29]..... 73

# 1 Introduction

## 1.1 Motivation

Currently, nanostructures are commonly fabricated using techniques such as photolithography, electron-beam writing and X-ray lithography. Although these methods are proven technologies that provide high-quality outputs, there are inherent problems. These techniques are generally expensive, slow, and the production of large patterns is difficult. Micro-contact printing ( $\mu$ CP) is a promising technology in which a patterned elastomeric stamp is used to transfer patterns of self-assembled monolayer (SAMs) onto a substrate by conformal contact printing. In 2008, a group of MIT students developed a high throughput, low cost roll-to-roll (R2R) printing technique into micro-contact printing, achieving good results. They also built a prototype machine to realize the whole process in the speed of 400 feet per minute while maintaining good quality outputs.

However, the last year's machine is only limited to printing octadecanethiols, an organic ink, on gold substrates where the self-assembly characteristics (see section 2.1) of these media could tolerate big range of pressure variance applied on the substrate. Therefore, if the micro-contact printing is applied into some other media where self-assembly characteristics do not exist, a highly uniform pressure along the substrate will be critical to the quality of outputs. The pressure of previous prototype machine is provided by the contact of the print roller and the impression roller. The uniform roundness and straightness of the rollers is key to the uniform pressure along the contact area. Meanwhile the parallel contact between the impression roller and the printer roller is also very important. Therefore, if we can fabricate the print roller with the variance less than a few microns and the contact between the impression roller and the printer roller has good parallelism with high repeatability, then the roll-to-roll micro-contact printing technology could be easily applied to various printing media.

The printer roller consists of central shaft, sleeve, the backing plate and the stamp (see section 2.2). The uniform thickness of the stamp is the most critical component of the uniform roundness of the print roller. Currently, there is no standard process to fabricate the stamp with the thickness variance of a few microns, therefore, the repeatable, reliable and manufacturable stamp fabrication process is also highly desired.

Another limitation of last year's project is that the registration of multiple layers on a flying substrate was not considered; only monolayer could be printed using the prototype machine. However, in the industry, multi-layer printing is required, which

means to print another layer on the substrate with patterns. At present, the commercial printing industry, where multi-layer printing is very common and popular, can only achieve a resolution of 40 microns. Thus, such technology can hardly be applied to multi-layer printing where the pixel size is less than 40 microns. If multi-layer printing with the resolution of 1 micron could be demonstrated by upgrading the previous prototype machine, there will be a significant impact in the printing industry.

Research was funded by and in cooperation with Nano Terra Inc, a Cambridge, Massachusetts company that specializes in Soft Lithography.

## **1.2 Problem Statement**

The primary objective of this project is to address the limitations of the previous prototype machine in related to the potential manufacturing of printed electronics using micro-contact printing technique within the soft lithography (SL) field.

At first glance, the main goals of this project can be split in two major areas:

Improve the printing quality, upgrading the R2R system built by the MIT students in 2008; in particular this goal will be achieved by designing and fabricating an interchangeable stamp on the roller that allows a quick replacement of the stamp once it is used up, without losing of alignment. This goal is achieved by performing three key steps:

- Design of an interchangeable stamp.
- Fabrication and demonstration of interchangeable stamp.
- Test results providing data on distortion, and alignment.
- Budget estimate for manufacturing applications.

The second main goal of the project is to improve the overall R2R system. This task is achieved by executing the following steps:

- Redesigning and implementing the impression roller system.
- Designing process for multi-layer printing
- Designing a high precision positioning system.
- Test results providing data on distortion and alignment.
- Budget estimate for manufacturing applications.

### 1.3 Primary Analysis

We considered the two major goals of the project, namely, fabricating a very flat stamp and then wrapping it around the print roller, and proving that micro-contact printing can be used for printing multiple layers with alignment.

In order to fulfill these goals, our approach consisted of accomplishing the followings:

1. Flat stamp fabrication. To achieve this, a new method was developed to fabricate the stamp using a molding process, to ensure a flat and defect-free stamp.
2. Wrapping the stamp with backing plate onto the roller with alignment and repeatability. The goals of this process were to wrap the stamp while maintaining alignment, and developing a repeatable process; and to maintain uniform roundness of the stamp after wrapping. To achieve this, after looking at a lot of options, we decided to use a magnetic cylinder, and a pin-slot system to grab the edge of the backing plate. We also considered a fixture system to wrap the stamp with backing plate on the cylinder.
3. Ensuring the roundness of assembled print roller within 4 microns tolerance. With proper wrapping method, minimal and uniform printing pressure could be achieved and hence realized good printing quality.
4. Redesigning the impression roller system to improve its repeatability of parallelism. In this process, we built up error budget model, found out the constraint to the repeatability of the impression roller system and then updated the system.
5. Designing a high precision position system to control the print roller position and orientation. This step was fundamental to improve the quality of single layer printing as well as the multiple layers printing.
6. Printing using the updated machine and comparing results that achieved by last year's group. After we qualified the wrapped stamp and impression roller system, we mounted the new roller onto the current machine, to get a direct comparison of print quality.

7. Printing multiple layers as a proof of concept. This was an independent step, to prove that micro-contact printing can print multiple layers on a single substrate with minimum misalignment.

## **1.4 Scope**

Our project only dealt with micro-contact printing with PDMS as the stamp and 300mm wafer as the master. We focused on printing thiol onto gold-coated substrates. This scope allowed us to decide the dimensions of our design based on available materials. The mature printing mechanism also allowed us to verify our designs without disturbance of different printing conditions.

For multi-layer printing, the initial purpose was to use rigid and transparent material (glass) as the substrate to print two layers using the same stamp to print twice. Later on, the scope switched to using updated R2R machine to print two layers with the same stamp in order to demonstrate what is the best alignment can be achieved using current Roll-to-Roll technology. In order to achieve this target, precise control of the printer roller on its alignment is required and we assumed the motion of the flexible substrate is self-aligned across the printing direction.

## **1.5 Task Division**

This thesis is based on a team project executed as part of the Mechanical Engineering Master of Engineering in Manufacturing Degree Program. The team members were:

Wenzhuo Yang has researched and determined the measurement methods for cylinder roundness, tolerance of stamp fabrication parts as well as the print quality of output features. He designed the measurement structure and analyzed the data obtain from both measurements. In addition, he worked with Yufei Zhu on the upgrade of impression roller system and multi-layer printing process design.

Paolo Baldesi has designed the high precision positioning system to control the position of the print roller. He calibrated the system and determined its performance. In addition, he worked with Charudatta Datar in developing an innovative wrapping process designing a new magnetic print roller. He also researched and designed the mechanism of growing UV-curable material onto cylinder directly.

Charudatta Datar has designed the magnetic roller, and developed the technique to attach and wrap the backing plate and PDMS stamp onto the print roller. He also worked with Paolo Baldesi in designing the high precision positioning system. In addition, he designed other components, compatible the high precision positioning system, to mount the new print roller on the machine built by the MIT '08 team,.

Yufei Zhu designed and constructed the multi-layer printing machine. He also designed the stamp fabrication parts with Mr. Werner Menzi from Nano-terra Inc.

We collectively tested the machine and determined the quality of printing resulted from the machines. Since we were working on a common project, the first three Chapters of our individual theses are common. Moreover, Chapters 7, 8, and 9 are common for Paolo Baldesi and Charudatta Datar. Chapter 7 and 8 are brief introductions to Zhu, and Yang's parts, while Chapter 9 discusses the conclusions of the project and possible future works.

## 2 Literature Review

This section summarizes the existing R2R machine developed in 2008 by Adam Stagnaro, Kanika Khanna, and Xiao Shen <sup>[4,20,21]</sup>, introduced the technologies used in the machine, and described its structure, function, operation steps and the result achieved. Also some pioneering studies of the currently multi-layer printing technology were reviewed to enlighten our prototype design on current R2R machine. Finally, some popular and representative optical metrology systems are studied to search out proper methods for measuring the quality of the machine design and the print output.

### 2.1 Soft Lithography

Photolithography is a well-established micro-fabrication technology, being widely used to manufacture most integrated circuits. It is, however, limited to a feature size of about 100 nm owing to optical limitations. Technologies such as extreme UV lithography, soft X-ray lithography, electron-beam writing, focused ion beam writing, and proximal-probe lithography <sup>[1]</sup> are capable of manufacturing smaller features, however, they are limited by high cost and technology development.

Photolithography also has other limitations: it cannot be used on non-planar surfaces; it is incapable of producing three-dimensional structures, and it is not suitable for generating patterns on glass, plastics, ceramics, or carbon [1].

Thus, a family of techniques called as soft lithography, including, microcontact printing, replica molding (REM), microtransfer molding (mTM), micromolding in capillaries (MIMIC), and solvent-assisted micromolding (SAMIM) are emerging as prospective solutions to overcome some of the limitations of photolithography.

They offer a number of basic advantages, such as, little capital investment, and simplicity. Apart from these, soft lithography techniques can produce features smaller than 100 nm, with relatively simple technology, and they are not subject to optical limitations. They also offer flexibility in terms of surface material, and shape, overcoming some of photolithographic limitations.

These techniques are referred to as “soft lithography” because each technique makes use of flexible organic materials as opposed to rigid materials to achieve pattern transfer to the substrate. Basically, these techniques involve the fabrication of an elastomeric stamp (typically made of Polydimethylsiloxane, PDMS), generating a replica

of the pattern originally on a Silicon master, and using this stamp to print the pattern on a substrate using self-assembly.

Self-assembly refers to the spontaneous formation of molecules into organized structures by non-covalent forces. The resulting structure is highly uniform, defect-free owing to thermal equilibrium, and in the lowest energy form.

Self-assembled monolayer (SAM) is one such non-biological self-assembly system (see Figure 1 for its process). SAMs is used in soft lithography to transfer the pattern on the elastomeric stamp, onto the surface of the substrate using minimal contact pressure.

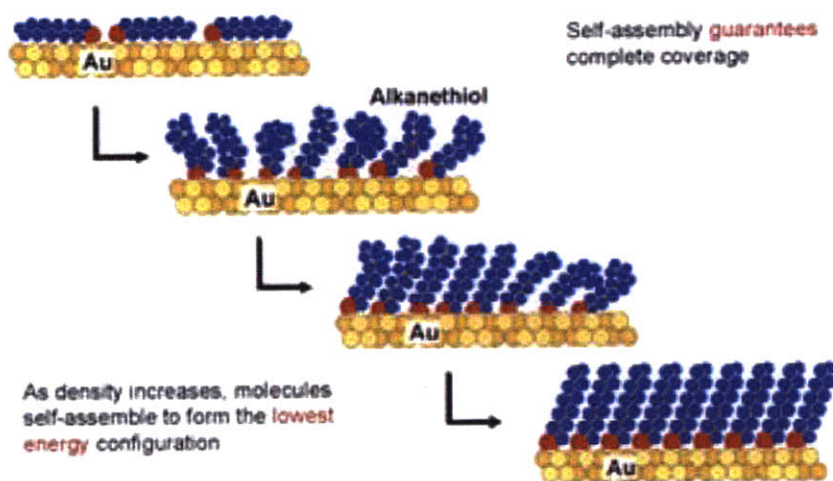


Figure 1: Illustration of The Self-Assembly Process<sup>[2]</sup>

We emphasize one of soft lithography techniques, microcontact printing, because we used this method throughout the project. This thesis does not describe the other methods.

## 2.2 Micro-contact Printing

The micro-contact printing process involves transferring a pattern on an elastomeric stamp onto the surface of a substrate by the formation of a monolayer of ink, which can be used as resist in subsequent etching, or other steps. This process relies on SAM, in which it enables transfer of only a monolayer of ink to the substrate. This molecular level contact makes the process independent of excessive ink being trapped between stamp and substrate, allowing significantly smaller sized ( $\sim 50$  nm) features to be printed onto the substrate.



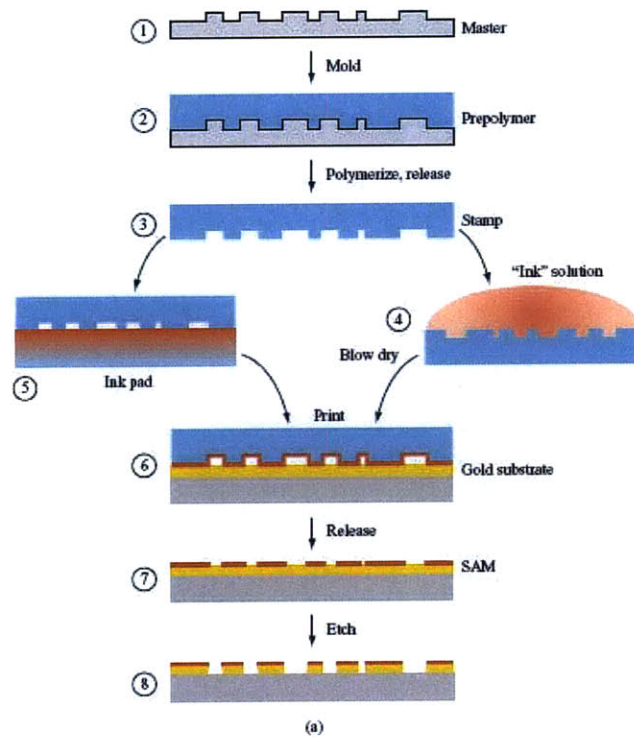


Figure 2: Steps Involved in Micro-Contact Printing <sup>[3]</sup>

The micro-contact printing process, as shown in Figure 2, involves, like all soft lithography techniques:

1. A master with the original pattern on it. This is typically a patterned Silicon wafer.
2. This pattern is then replicated on a PDMS stamp by casting or molding.
3. This PDMS stamp is then inked, by a couple of methods (using an ink pad, or pouring ink over the stamp).
4. Next, this inked stamp comes into contact with the substrate that is to be printed upon.
5. This contact enables the formation of a SAM of the ink on the surface of the substrate.
6. The stamp is released, and the SAM formed on the substrate is then used in subsequent etching steps to generate the required pattern on the substrate.

## 2.3 Existing Roll-to-Roll Equipment

The MIT'08 team's (Adam Stagnaro, Kanika Khanna, and Xiao Shen<sup>[4,20,21]</sup>) task was to take this demonstration to the next level, and prove that the paradigm would be competitive with commercial printing systems in at least one of the parameters - quality, rate, flexibility. The key goal of this MIT'08 project was to achieve Micro-contact printing at very high speeds (400 ft/min), on 8" wide coated substrate (web).

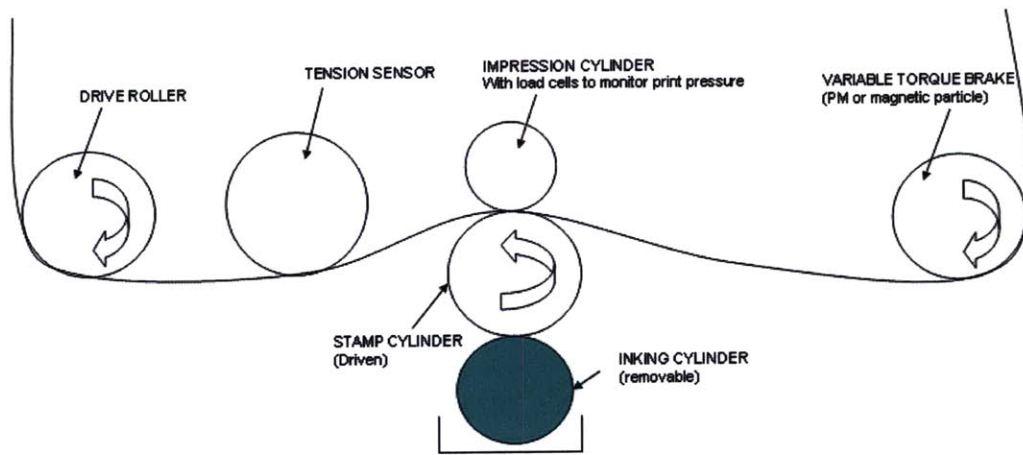


Figure 3: Concept of The Machine<sup>[4]</sup>

The concept of the machine is shown in Figure 3. The substrate was in the form of a web, driven through a set of rolls. A combination of open and closed loop using motors and clutches was used to achieve tension control.

The equipment can be divided into three modules:

1. Supply Module (to unwind substrate web).
2. Print Module (to ink, print, and apply pressure).
3. Collect Module (to rewind substrate web)<sup>[4]</sup>.

The Figure 4 shows the layout of the machine, in terms of these three modules. The entire roller system is cantilevered about a common base plate. And Figure 5 shows the physical appearance of the R2R machine built by 08' group.

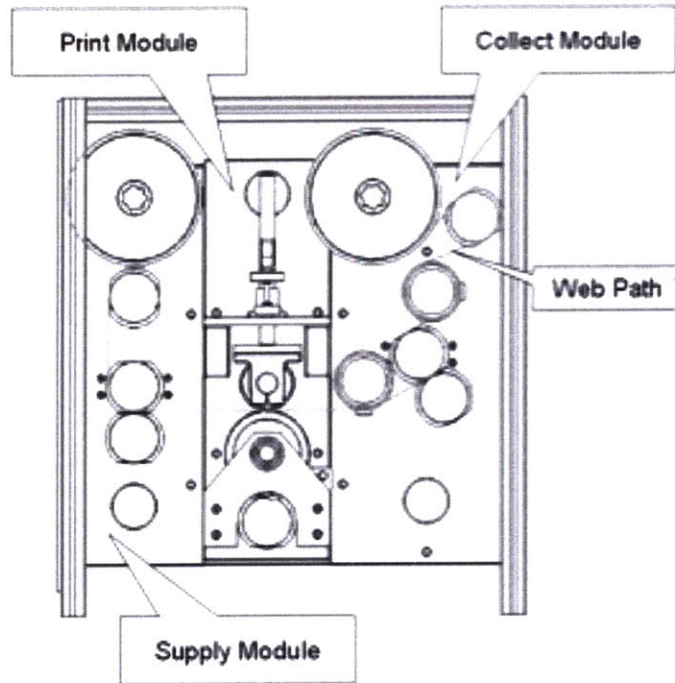


Figure 4: Layout of The Three Modules in The Equipment <sup>[4]</sup>

We shall not describe the operation of the machine in much detail, but will emphasize on the results of the print module only, as this was felt to have the most significant impact on the results, which also have been described in detail later in this document.

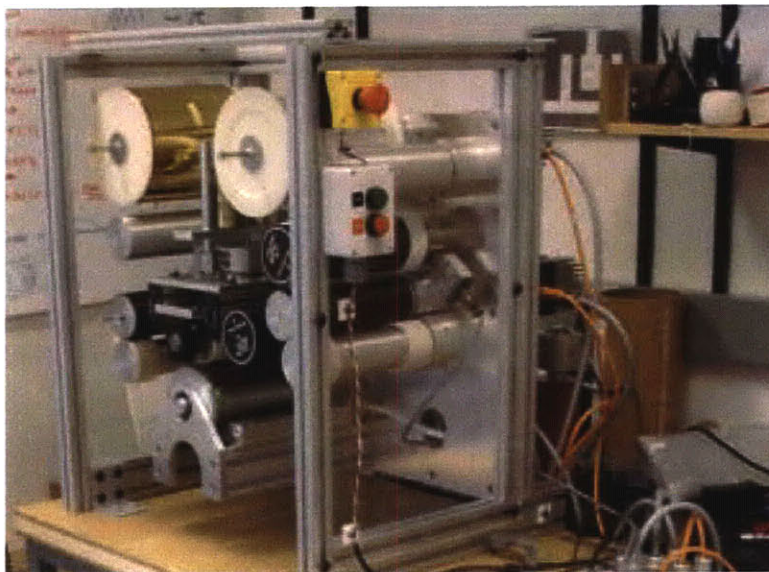


Figure 5: The R2R Machine Built in '08 [4]

A series of experiments were designed and conducted to test the printing quality. Below is a summary of relevant results <sup>[4]</sup>:

1. Neither printing pressure nor speed was found to have a significant effect on spatial distortions and pattern dimensions in the range of settings we used.
2. It is possible to print a robust etch-resisting SAM at very high speeds (400 ft/min, unit area contact time  $\sim 5$ ms).
3. At very high speeds (400ft/min), some systematic air trapping was observed
4. The alignment of the stamp on the backing may have a significant effect on distortion patterns.

These results have formed the basis for our project. Improvements in the following were seen as critical to improving the printing quality:

- Alignment of the stamp on the backing, and therefore on the print roller.
- Fabrication of a flat stamp.
- Precision in the web handling system of the equipment.

## 2.4 Stamp Casting Machine

Stamp fabrication is essential to improve the quality of printing. Micro-contact printing requires precise transfer of patterns with minimum distortion and maximum yield. In addition, the stamp needs to maintain an exactly complementary pattern to the master, and it should avoid distortion during printing.

PDMS as the material for stamp has a low Young's modulus; therefore, under tension or external force, the PDMS will distort and result in a distorted pattern. In previous projects, PDMS has been cast onto a rigid backing plate. The backing plate is treated with a plasma and surface treat chemicals to increase its adhesion to PDMS, and the force between this backing plate and PDMS is firm enough that little relative motion between the stamp and backing plate will happen. Thus, the backing plate with PDMS minimizes distortion when wrapping the stamp onto the print roller.

With the consideration of cost and efficiency, large stamps are desired for production. In common practice, round wafers (150mm, 200mm and 300mm size) are used as the master and etched out negative pattern on the SU-8 layer on the master. This photo-resist will directly contact PDMS during the practice, thus caution should be made in order not to destroy the pattern on the master. The size of the stamp is limited by the size of wafer. In this project we targeted 300mm wafer as our master and

explored the problems including distortion, uniformity, peeling force from master and repeatability with the capability of scaling in manufacturing.

In previous research at Nano-Terra LLC, the thickness of the stamp was shown to affect the pattern transfer and a thin stamp seems to result in better printing quality. This research is not restricted to self-assembly monolayer printing, For applications in which pressure is critical to the quality and yield of printing, the elasticity property of the stamp will be key consideration and this property is directly affected by the thickness of stamp. A uniform, thin layer of stamp is beneficial to other on-going projects in the soft lithography.

Nano-Terra developed their first casting machine (see Figure 6) using aluminum with a 12" master, which demonstrated capability of large area stamp fabrication. In Figure 6, a vacuum chuck at the left hold the backing plate and flips onto the wafer chuck at the right where the wafer sits. PDMS is injected into the gap between backing plate and wafer.

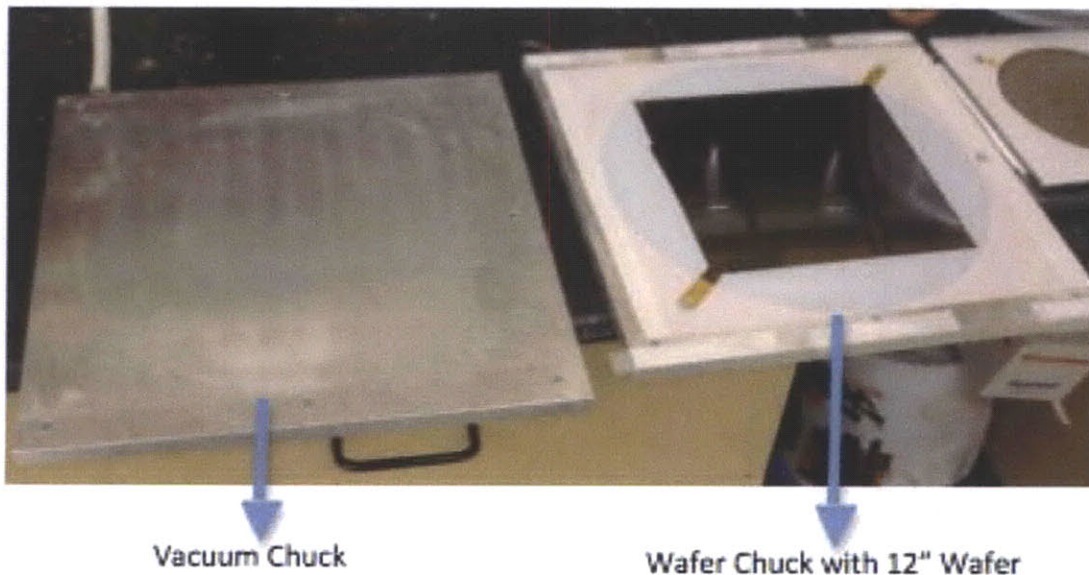


Figure 6: Main Parts of Aluminum Casting Machine for Large Area Stamp, Developed by Nano-Terra LLC.

As shown in Figure 6, this configuration is to have two vacuum chucks: one attaching the master and the other attaching the backing plate. A dam (or reservoir) is placed around the area. These two chucks face each other, and create a space, which is circled by the dam. Liquid PDMS is injected into the area with a syringe.

This pilot stamp fabrication equipment demonstrated consistent quality for use in large size stamp. However it is not designed for interchangeable masters because its

mechanism for fixing the master does not allow quick uninstal. Also the space between backing and can't be adjusted easily. Thus it was not able to experiment for manufacturing purpose. Surface finish of the vacuum chuck is rough, which results in uniformed thickness across the stamp.

To resolve these problems identified from this pilot PDMS casting machine, a better material that is capable of ultra-high precision machining is necessary. The Wafer chuck will be modified to add-in alignment capability for maintaining repeatability each time a new master is brought in. Thickness of stamp can be varied by changing the spacing part between wafer and backing plate. This is the topic of Yufei Zhu's thesis <sup>[24]</sup>, detail explanation on stamp fabrication process could be found in his thesis.

## **2.5 PDMS Peeling Process**

The peeling process is a crucial step where we need to wrap a PDM stamp, which initially lies flat on a Silicon wafer, onto the print roller. Thus, it is essential to first successfully peel the PDMS stamp without any tears or distortions. This section studies some of the research that has been done on peeling PDMS off Silicon wafer.

### **2.5.1 Stress Zones at PDMS Peel-Front**

Considerable research has been done on peeling PDMS off a Silicon wafer. However, the upper side of PDMS is not attached to any other surface (like a metal plate), but is open to air. In our project, the topside of PDMS is attached to a steel backing plate. However, some of the findings of the research are indeed useful despite this difference, and are as below.

In general, at the peel front, boundary conditions are different on the two sides of the PDMS stamp; in fact, on one side, the surface of the film has zero shear stress (or very small shear stress, in our case) because it is not attached any surface (or to a different surface), while on the other side, the film adheres to the silicon master and shear stress is imposed on it by the substrate. This configuration creates a singularity around the peel front. This very small and thin zone is characterized by a highly variable stress values. This stress singularity in the normal direction causes the separation of the film at the peel-front.

When viewed closely to the peel front, peeling of PDMS could be schematized as in Figure 7:

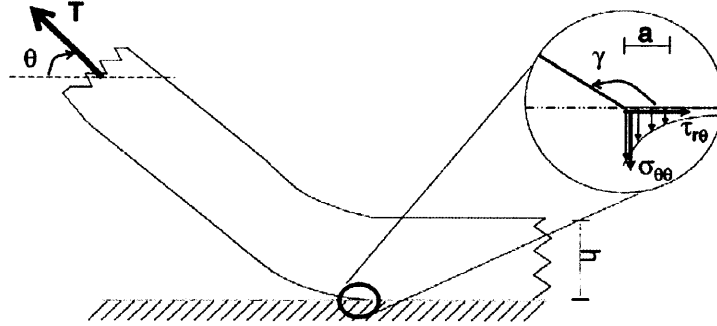


Figure 7: Illustration of Separation at The PDMS-Silicon Wafer Boundary <sup>[22]</sup>

### 2.5.2 Initiating Peeling

Generally, to initiate the peeling operation we need apply a force at the peeling front, and as shown in Figure 8, this force can be applied either, A: an upward force on the top surface of the film or B: a force applied at the edge on the bottom surface. Previous works showed that, the success of either approach depends on how close the applied force is to the vertical plane of the peel-front. Only when the force is applied in the same vertical plane as the edge, the singularity at the edge results in peel-initiation.

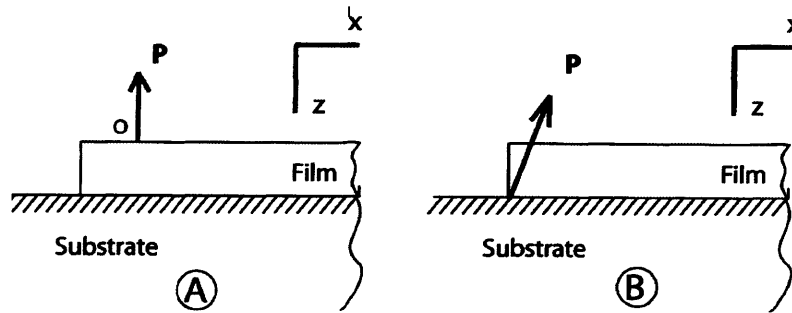


Figure 8: Directions of Peeling Force <sup>[22]</sup>

## 2.6 Multi-Layer Printing

After the successful demonstration of high throughput and good yield in one-layer printing using R2R machine, our background knowledge is sufficient to start the research in micro-contact printing's capability of multi-layer printing. This is an important step towards the actual application in manufacturing because micro-contact printing is no longer limited to printing of photo-resistive material as the ink. Further applications require multiple layers to overlap to achieve complex function. The units under consideration include diodes and transistors with at least 3 layers.

An important specification introduced in multi-layer printing is accuracy in relative layer position or registration. We are expecting to achieve registration with the roll-to-roll structure, because of the high throughput. However most literature discusses methods to align surface to surface, including the alignment between mask and wafer in semiconductor industry, or dip and substrate in inkjet printing, while few have mentioned alignment issue between round subject and flat substrate. Thus references for designing machine capable of multi-layer printing will be mainly from color printing industry.

It is common practice to start building high precision system based on an open-loop structure and to add-in close loop component to increase the accuracy. An open-loop structure is simple because micro-contact printing requires only two motions: linear motion of substrate and rotational motion of the print roller. Since roll-to-roll machines are widely used in printing industry, it is beneficial to learn how the feedback systems work. We will use gravure printing to demonstrate how the printing industry achieves this registration. Figure 19 shows a typical gravure-printing machine.



Figure 9: Gravure Printing Machine.



Gravure is widely used in high quality printing. Because human eyes are not sensitive to features less than 40 micron wide, the feedback system for gravure machines usually sets the accuracy at 100 micron or less. Errors in two key directions have been compensated. One is the direction of substrate motion during printing, or the “path”; the other is the direction perpendicular to the path on substrate plate. The latter is easy to adjust by moving roller along its axis; the error in path is sensed and compensated using sleeve displacement between the roller and the sleeve (see Figure 10).

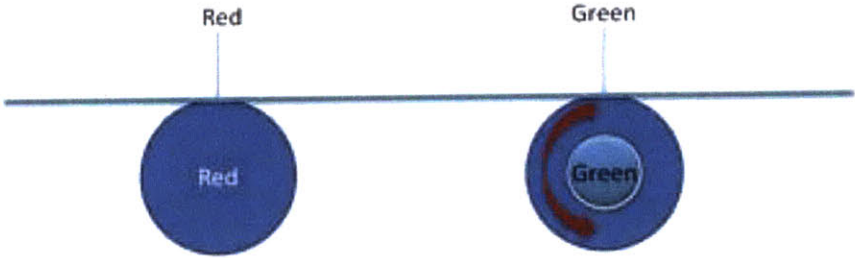


Figure 10: Actuation Method For Adjusting The Relative Distance Between Print Nips on The Substrate.

In Gravure printing, marks are printed with a distance of 20mm, and individual roller prints each color mark. Sensors are used to check the distance between marks to determine the relative position between different colors on substrate. The sensor system is shown in Figure 11. The signal from sensors are received only when designated color are about to arrive. Once an error is detected, the controller will send out signals to the roller whose color is offset from its desired position, and the sleeve on the roller will rotate to compensate for this error.

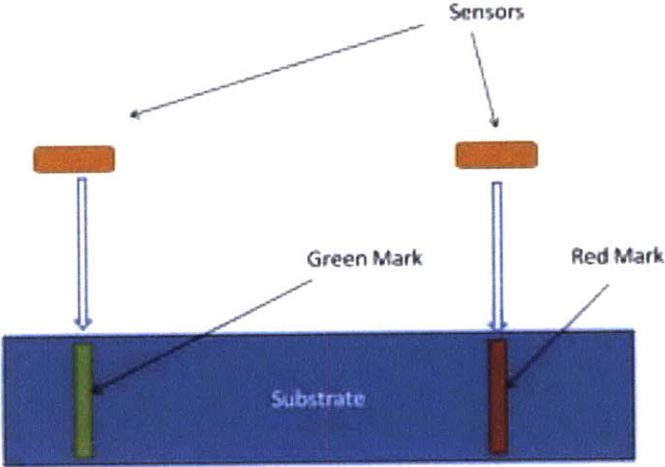


Figure 11: Simplified Sensing Method For Detecting The Relative Position Between Two Layers of Print in Gravure Printing.

Assume both red and green rollers are rolling at the same speed, the green and red mark on the substrate will have a constant distance of 20mm, and signals from both sensors will reach controller at the same time. If, however the green roller is one step behind compared to the red roller, the green mark will shift back at some distance, and a signal from the green sensor will lag from the red signal. The controller will determine the amount of offset from the time of this lag and control the sleeve on green roller to shift one step ahead.

## 2.7 Optical Methodology System Review

One of the objectives of the project is to fabricate the stamp within the variance of  $\pm 4\mu$ , which means high precision measurement tools has to be employed. Currently, there are various kinds measurement sensors that can achieve very high accuracy and resolution, but they also have specifications that match some specific needs. In this section, laser triangulation sensors, interferometers, fiber optic sensors and con-focal microscopy are reviewed as our potential choice of measurement sensors.

### 2.7.1 Laser Triangulation Sensors

Triangulation measurement is an old but very useful method to measure distance. Laser sensor is a powerful tool, using triangulation measurement, to measure either long-distance or short-distance with high accuracy. However, the long distance measurement may not provide very high resolution. Laser sensor projects a spot of light onto the target and receives the reflected light with photo detector through an optical lens. A typical laser triangulation system is shown in Figure 12 below.

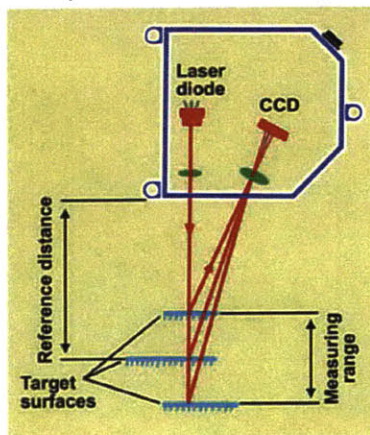


Figure 12: Principal of Laser Triangulation Sensor [14]

From the Figure 12, we could see that the relative position of laser diode, lens, photo detector and the position of reflected light from the target on the photo detector determine the distance of the target. If the target changes its position, the reflected light changes its position on photo detector as well. Through linearization and additional digital or analogue signal processing, the detector could provide an output signal proportional to the position of the target. The ambient light has little effect on reading, because the signal is proportional to the center of intensity of focused image <sup>[14]</sup>.

The most important part of laser sensor is the photo detector, which could be photo diode, position sensitive device (PSD), charge coupled device (CCD), Complementary metal-oxide-semiconductor (CMOS), etc. Different photo detector requires different signal processing method.

The following summary of general laser triangulation sensors' characteristics is built upon the works done by Alexander H. Slocum in his book named *Precision Machine Design* <sup>[15]</sup>, updated with recent industry standards. Note that the manufacturers are always advancing the state-of-art, so this summary is generalization only.

- **Size:** Typically 30x50x70mm.
- **Cost:** Depends on the resolution. Normally, 1  $\mu$  resolution laser sensor cost \$4000.
- **Measurement Range (span):** 3 - 1300mm.
- **Accuracy (linearity):** 0.03% of Span, 500 Hz, to white target (85% diffuse reflectance).
- **Repeatability:** Depends on the repeatability of the surface finish.
- **Resolution:** on the order of 0.005% of full-scale range, could achieve as high as 0.1 $\mu$ m.
- **Laser spot size:** 30-300 $\mu$ m.
- **Environment Effect on Accuracy:** On the order of 0.01%/<sup>o</sup>C of full-scale range from the nominal 20<sup>o</sup>C operating temperature.
- **Power:** 15 – 24 Volts DC, 120 – 200 mA draw with 350 mA surge at power-up.
- **Allowable Operating Environment:** Keep optical windows clean for best performance. System typically operates from 0 to 40 <sup>o</sup>C.

### 2.7.2 Interferometer Sensors

Various kinds of interferometers are in use today. Michelson interferometer has the most common configuration for optical Interferometry and was invented by Albert

Abraham Michelson. A typical and simplified interferometer system is shown schematically in Figure 13.

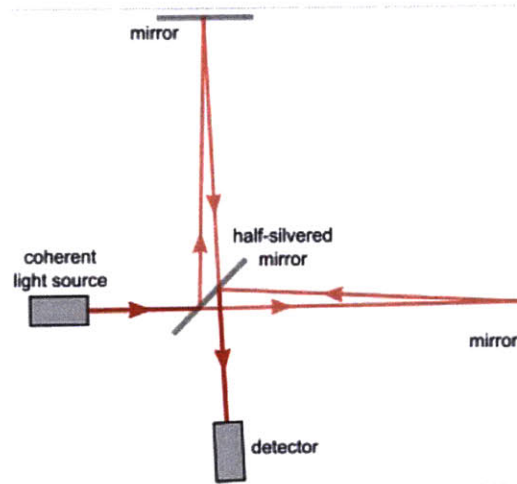


Figure 13: Principal of Interferometer System [15]

According to Figure 13 a continuous light source was spitted into two paths: One bounces back from the semi-transparent mirror, and then reflects back from the mirror on the top, goes through the semi-transparent mirror, to the detector. The other one goes through the semi-transparent mirror, bounces back from the mirror at right, and then reflects back by the same semi-transparent mirror and goes into the detector. Difference in path may result from the length difference or different materials, which cause alternating pattern on the detector. If no difference of materials involved in the interference, the distance could be measured through.

The following summary of general laser triangulation sensors' characteristics is built upon the works done by Alexander H. Slocum in his book named *Precision Machine Design* <sup>[15]</sup>, updated with recent industry standards. Note that the manufacturers are always advancing the state-of-art, so this summary is generalization only. It is also extremely important to stress that the accuracy of measurement is highly depended to the manner of how the optics are mounted and how the environment are controlled.

- **Size:** Laser head, 130x180x530mm.
- **Cost:** About \$9000 for laser head and electronics boxes for up to 4 axes of measurement.
- **Measurement Range (span):** up to 30m<sup>[16]</sup>.

- **Accuracy:** In a vacuum, if perfectly aligned, the accuracy can be on the order of half (worse) the resolution. As for non-vacuum conditions, the environment significantly impacts the accuracy of measurement.
- **Repeatability:** Depends on the stability of the environment and the laser head.
- **Resolution:** Depends on optic used and can be achieved as high as  $\lambda/4096$ . Higher resolution could be achieved through better optics and phase measurement technique involved.
- **Environment Effect on Accuracy:** About  $1\mu\text{m}/\text{m}/^\circ\text{C}$  Air turbulence and thermal expansion of optics, mounts and the machine itself <sup>[16]</sup>.
- **Power:** 12 V, 200 mA (PICO M8 con.).
- **Allowable Operating Environment:** Since the interferometer is sensitive to the environment, ideally, it should be used in a vacuum, or in air of  $20^\circ\text{C}$  with no gradients.

### 2.7.3 Fiber Optic Sensors

Optical fibers are glass or plastic fibers that transmit light using the property of total internal reflection and the fiber act as waveguide. Figure 14 demonstrates the total internal reflection of a laser inside the optical fiber.

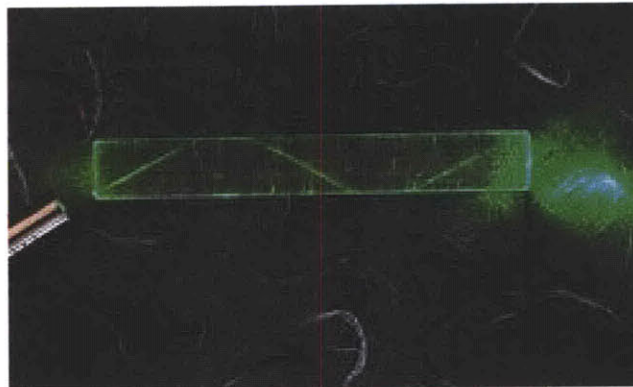


Figure 14: Total Internal Reflection inside Optical Fiber [15]

The key elements for fiber optic sensor are two sets of flexible probes: one is for transmitting and the other is for receiving. Two probes are jacketed into one to measure the distance. There are basically three kinds of probes configurations: Hemisphere,

Random and concentric, as shown in Figure 15. Active diameter of probes could be as small as 0.177mm, making them ideal to measure small target [17].

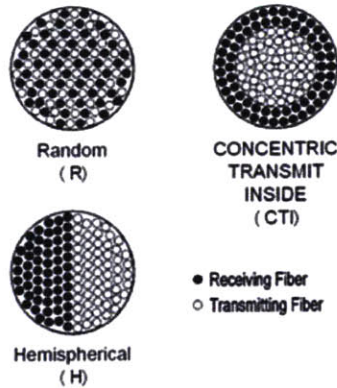


Figure 15: Fiber Optic Probe Configuration [17]

The distance of an object can be determined based on the intensity of reflected light that is sensed by two transmitting and receiving fiber probes [18]. The response curve is shown in Figure 18, and the intensity of reflected light is converted to voltage output. Optic Fibers are not sensitive to electromagnetic interference and typically very light [16].

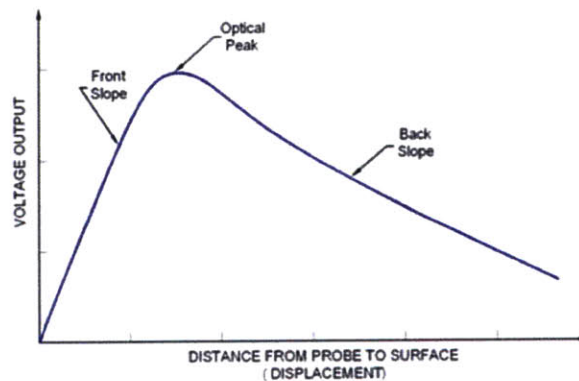


Figure 16: Fiber Optic Probe Response Curve [17]

The following summary of general laser triangulation sensors' characteristics is built upon the works done by Alexander H. Slocum in his book named *Precision Machine Design* [15], updated with recent industry standards. Note that the manufacturers are always advancing the state-of-art, so this summary is generalization only.

- **Size:** cable diameter could be 1mm or even smaller.

- **Cost:** Depends on the type of sensor, \$100-\$1000.
- **Measurement Range (span):** a few millimeters for small displacement (<10mm).
- **Accuracy:** 0.1% of full range.
- **Repeatability:** Depends on environment conditions.
- **Resolution:** Can achieve very high resolution if the sensor held very close to the target, like 0.01 $\mu$ m resolution with the range of 0.1mm.
- **Environment Effect on Accuracy:** very sensitive to environment, like dirt on the sensor will degrade the performance.
- **Allowable Operating Environment:** Since the interferometer is sensitive to the environment, the sensing surface must be kept very clean. Individual probes should be kept away from moisture, or they will eventually erode to the point of failure.

#### 2.7.4 Con-Focal Laser Scanning Microscopy

Con-focal laser scanning microscopy (CLSM or LSCM) is a technique that could capture high-resolution optical images with high selectivity of the height <sup>[23]</sup>. A very important feature of con-focal microscopy is that it could obtain in-focus images from various depths. Because of its high resolution on depth measurement, the con-focal microscopy could be applied to measure the flatness of object within the limitation of the measurement tool.

In con-focal laser scanning microscopy, a coherent light source projects a beam of laser, which goes through the beam splitter and focused on the target via lens. Scattered and reflected laser light, together with the illumination light, were re-collected by the lens and then focus on the detector via the reflection of the same beam splitter. The aperture of detector blocks the light that is not from the focal point and hence leads to a sharper image comparing to conventional microscopy (Figure 17).

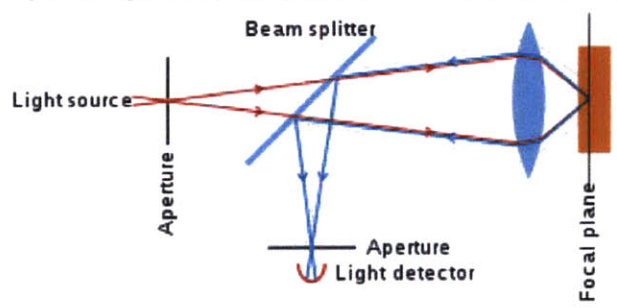


Figure 17: Principal of Con-Focal Microscopy [23]

Adjusting the position of lens could allow light detector capture the sharpest image of the targeted area. Most of current con-focal measurement systems are using CCD to detect the target and measure its position.

In this project we are using Nikon VERITAS VM250 as our main metrology to test the surface flatness through measuring the depth of the sample points. The following is the summary of general characteristics of Nikon VERITAS product series.

- **Size:** Main body - 565 x 690 x 740 mm (minimum height), 72kg; Controller - 145 x 400 x 390 mm, 13kg.
- **Cost:** Depends on the type the precision and measurement range, more than \$10,000.
- **Measurement Range (span):** could achieve 50mm.
- **Accuracy:** could achieve 1  $\mu\text{m}$ .
- **Repeatability:** rely on xyz moving stages.
- **Resolution:** Can achieve 0.1 $\mu\text{m}$ .
- **Power:** AC100-240V $\pm$ 10%, 50/60Hz.
- **Environment Effect on Accuracy:** within allowable operating environment, the accuracy can be well maintained.
- **Allowable Operating Environment:** Temperature - 10°C to 35°C; Humidity - 70% or less.



### 3 Methodology

#### 3.1 Stamp Casting Machine

Before processing the casting machine compatible with 12" master, we started with a 6" casting machine to see the capability of the design and building material (316 Stainless Steel). The design allows both 150mm wafer and 200mm wafer to be used in the same configuration. The stamp-casting machine will be capable of alignment for different masters. We use pins to locate wafer. In order to hold tight the wafer during pouring PDMS, grooves are designed for vacuum capability and wafer will be held using vacuum after aligning (see Figure 18). Because no glue or tape will be used in the process, wafer will be easily replaced once the vacuum has been turned off.

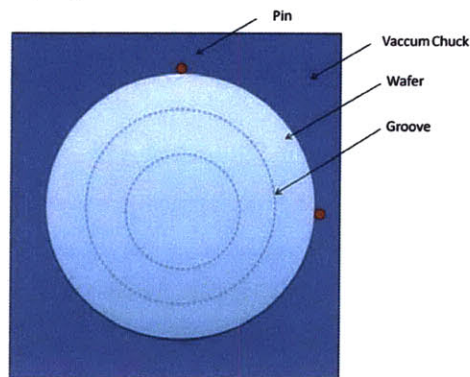


Figure 18: Structure for Wafer Chuck

A single piece of Teflon with a rectangular opening inside will attach to master as the dam for holding PDMS within the area, this Teflon will also act as spacer between master and backing plate (see Figure 19). This Teflon determines shape and the thickness of the stamp on the backing plate.

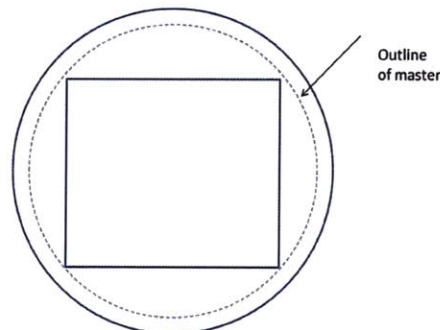


Figure 19: Teflon Spacer

The area for containing PDMS is confined by:

- Wafer on the top for transferring pattern.
- Thin stainless steel sheet (backing plate) sitting at the bottom as the backing for PDMS.
- Dam between wafer and backing plate for holding the PDMS.

Repeatability is the critical design specification. Under this configuration, making a single big stamp will require many identical steps, and each step will result in a small area of finished stamp. Variables to be considered are:

- Distance between master and backing plate (all attached to the chuck).
- Displacement between master and backing plate.
- Uniformity of the stamp.

All these variables can be decomposed in 6 dimensions: 3 linear and 3 rotational. A sidebar is used to align both chucks, as shown in Figure 20. The backing plate chuck (referred as SS Vacuum Chuck) is fixed to the side bar, while the adjunction of wafer chuck and sidebar leaves some clearance for adjusting. Minor adjustment is done by using screws to locate wafer chuck in both X and Y directions. The Z direction, also determines the height for stamp, is fixed by the thickness of dam.

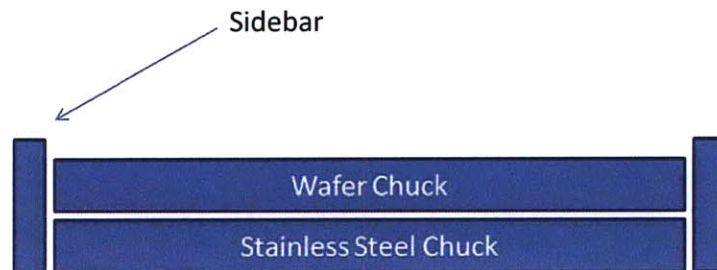


Figure 20: Sidebars Used to Align Both Chucks

Because the fabrication of stamp from PDMS is done in a low-pressure environment, the chucks with dam inside will be clamped together with strong force to ensure no air leaks in. Traditional C-clamp does not fit here because point contact will create distortion. Our approach needs to distribute the force as uniformly as possible. A clamping bar connected to sidebar by screw is used to provide clamping force. Small precision springs will be inserted between the clamping bar and wafer chuck to apply equal force.

## 3.2 Peeling and Wrapping the Stamp on the Print Roller

The R2R machine that was built by MIT'08 group proved that the R2R technique is feasible with micro-contact printing technology, but experiments showed that the printed images were affected by many distortions. The current way to wrap the PDMS stamp on the print roller is performed manually using a seam on the cylinder.

The challenges in the manual wrapping process using a seam demand the intervention of a skilled operator, making the process both time-consuming and labor-intensive. Also, even if all the operations will be performed in the correct way is not possible to guarantee the 5 microns alignment as required.

Therefore, the first goal of the project consists of improving the printing quality, designing a way to peel and wrap the stamp that will respect the following aspects:

- Maintain alignment.
- Fast replacement.

### 3.2.1 Gripping the Film for Peeling

The setup of the print roller before wrapping process is shown in Figure 21. This setup comes after flat stamp fabrication process: disassembling the vacuum chuck from the fabrication device and placing the print roller at the edge of the backing plate.

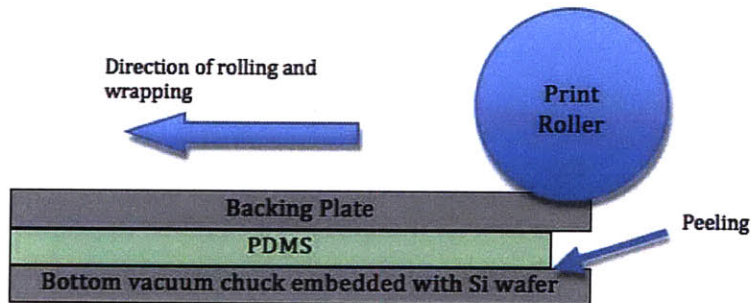


Figure 21: Illustration of Print Roller Setup before Wrapping

Any device that grips the backing plate for peeling off the stamp must accomplish three steps in the peeling process:

1. Initiate the peel.
2. Separate the film from the wafer.
3. Transport the peeled film away.

Unfortunately, the first and second stages are complicated by the inherent physics of peeling that we discussed in the literature review in the previous chapter. Let us begin by looking at the initiation of separation. This is a difficult step because the PDMS film adheres over the entire area of the substrate, leaving no 'lip' to hold the film or to start the separation. When an operator introduces a lip by inserting a razor, she must be careful not to scrape the film or inadvertently cut through it. Once she initiates separation, the operator may pull the film at point-contacts, which may cause excessive stresses and risk tearing around the contacts. If the film is adhered well to the substrate, she may need to pull hard on the PDMS film, which could also cause tearing.

Therefore, it is necessary to design a system that is able to grab and wrap at the same time the PDMS stamp that performs the following:

1. Grab the PDMS stamp without causing breaks or plastic deformations
2. Keep peeling the PDMS stamp applying a force with constant intensity, constant direction, and with a uniform distribution.
3. Wrap the PDMS stamp on the roller without losing alignment and without causing relative motion between cylinder and backing plate.

Keeping in mind the above requirements, we designed and analyzed concepts for peeling and wrapping the PDMS onto the backing plate. These concepts have been summarized below. It should be noted that, based on the results of the MIT '08 project, it is evident that this step of peeling and wrapping with precision and alignment is the most crucial step, in that it has a direct bearing on the printing quality.

### **3.2.2 Methods to Generate Adhesive Force Between Backing Plate and Print Roller**

Through the industrial investigation, we summarized the concepts, which is available on the market, to search for optimal solution the generate adhesive force between backing plate and the print roller:

#### *1. Electro magnet cylinder.*

It has ability to switch on and off the magnetic force of attraction, thus enabling better manual control over the pre-alignment of the print roller positioning with respect to backing plate. However, the electro magnet cylinder requires additional electrical components and needs complex additions or modifications to print roller.

#### *2. Permanent magnetic cylinder.*

It could provide strong magnetic force, even if rare earth magnets used, which is easily available. On the other hand, a permanent magnetic cannot switch off magnetic force. Also to machine a cylinder with permanent magnetic force is expensive and it is difficult to obtain precision in diameter.

*3. Cylinder with vacuum force.*

The vacuum holes along the cylinder could provide uniformly distributed attraction force along surface of cylinder. The vacuum cylinder is adaptable from existing commercial vacuum rolls. Nevertheless, the vacuum cylinder requires additional vacuum pump and vacuum control. And backing plate will have to cover entire vacuum-surface of cylinder; otherwise leakage of vacuum could be an issue.

*4. Cylinder with double sided adhesive tape on the surface.*

Attaching the double-sided tape onto the surface of the cylinder could also provide strong adhesive force and such design is obviously simple and easy.

The disadvantage of this method is that the double-side tape introduce another layer between the print roller and the backing plate which another source of variation on the roundness of the roller. In addition, it is difficult to correct errors of misalignment of backing plate with cylinder. Furthermore, cleaning cylinder for stamp replacement would be very difficult.

**Chosen Method:** Through analyzing above those possible solutions of the print roller, we finally decided to use stainless steel cylinder with a series of permanent magnets embedded into the cylinder. This kind of cylinder is a well-established design for use in the die-cutting and embossing industry, hence easily available. Also, this design satisfies all the precision and accuracy requirements with respect to the diameter, total run out, and straightness of the cylinder.

### **3.2.3 Methods to Wrap Backing Plate without Loosing Alignment**

*1. Slot in print roller, clamp to grab backing plate*

Clamp refers to an L shaped projection that would slip between the backing plate and the Si wafer. This would enable a positive grabbing or locking of the backing plate with the print roller, it requires pre-alignment before clamping.

*2. Slot in print roller, bent edge of backing plate*

This would be similar to using a clamp, except that the backing plate would be bent, and would stick out, enabling one to insert the bent edge into a slot in the print roller, again

accomplishing a positive locking arrangement. But the relative position of the edge of backing plate and the slot has to be very accurate in order to maintain the alignment.

### *3. Pins in roller, holes in backing plate*

This design consists of two (or more) pins inserted using threaded holes in the body of the cylinder. Corresponding holes would be drilled or machined in the backing plate. The height of the pins sticking out of the cylinder would be less than the thickness of the PDMS (less than 500 microns). This would prevent damage to the wafer during peeling and to the substrate during printing. Also the pins and holes could provide enough assembly constraints to guarantee desired alignment.

**Chosen Method:** Pins in roller, and holes in backing plate. This was found to be the simplest, easiest to adapt, and the most precise design.

#### **3.2.4 Analysis of Fixture System**

A fixture system that helps to guide the movement of the print roller during the wrapping was designed, as shown in Figure 22. The fixture would serve two purposes:

1. Pre align cylinder with backing plate.
2. Maintain alignment during wrapping of the backing plate on the cylinder.

However, the fixture system over constrains the cylinder-backing plate during wrapping. This is because, the force of adhesion between the cylinder and backing plate already achieves alignment between the two. Hence, if the fixtures try to achieve a slightly different alignment, it would create distortions and twisting forces in the backing plate, which would lead to detrimental effects on the stamp, and induce unwanted stresses in the stamp.

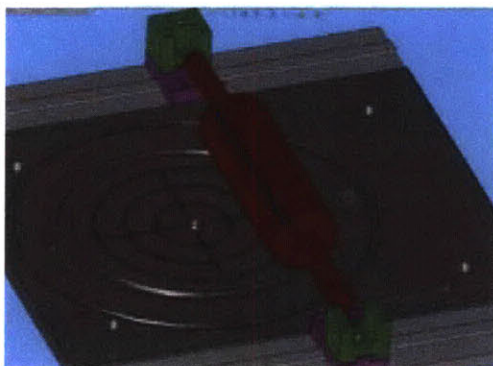


Figure 22: Illustration of The Proposed Fixture System

Upon conducting experiments with a prototype Aluminum cylinder, with pins, and holes on backing plate, and conducting error analysis for the same, it was decided that pin-holes are the best way to minimize alignment errors between the backing plate and print roller. Thus, the fixture system was not used.

### **3.3 Precision Measurement Method**

The initial goals of this project were to fabricate a stamp with uniform thickness, wrap the stamp onto the roller with uniform roundness and demonstrate multi-layer printing. In order to answer the questions such as how thick the stamp is, how flat the stamp is, how good the quality of multi-layer printing is and etc., a thorough measurement method needed to be developed to precisely and correctly answer those questions. Meanwhile, multi-layer printing requires upgrading the accuracy of alignment of the current R2R system, so a systematic measurement is also desired to demonstrate the improvement of alignment in accuracy.

#### **3.3.1 Flatness and Roundness Measurement**

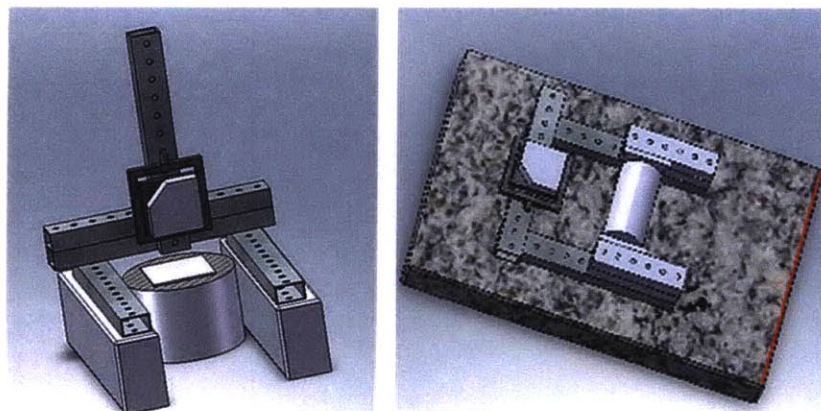
In the stamp fabrication and wrapping process, the ultimate goal is to make sure that the diameter of print roller has the variance of  $\pm 4\mu\text{m}$ , and the print roller here means the assembly of the central shaft, sleeve, and the backing plate with the stamp. All the potential variance could be broken down into following categories:

- Flatness measurement
  - Flatness of stainless steel.
  - Flatness of the PDMS stamp.
  - Uniform thickness of attached PDMS on stainless steel.
  - Flatness of devices that are used to fabricate the stamp.
  
- Roundness measurement
  - Roundness of print roller.
  - Roundness of central shaft.
  - Eccentricity of the motion of the driver motor.

Due to the specific characteristic of PDMS and the overall process, the measurement device should obtain following requirements:

- Non-contact measurement.
- High resolution, targeting on 1 $\mu$ m.
- Sufficient range (>1mm).
- Affordable.

At first, Laser triangulation sensor was the first choice, which is perfect aligned with all above requirements. Corresponding fixtures and frames were developed for the flatness and roundness testing, as illustrated in Figure 25. Basically, the laser sensor sits on the micrometer head for the fine adjustment and the micrometer head is mounted onto the frame to test either flat or round surface.



Flatness measurement

Roundness measurement

Figure 23: Fixtures for Flatness and Roundness Measurement

However, the chosen laser sensor cost more than \$4000 and could only be used for this project in the view of Nano Terra LLC, which is not cost effective for the company in sake of the future application. Therefore, we plan to use the available CNC Video Measuring Systems (Nikon VERITAS VM 250) that could measure the height of the surface by using con-focal technology. (The machine is shown in figure 24).

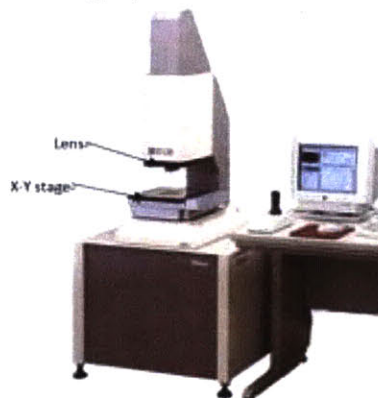


Figure 24: VERITAS VM 250



To measure the flatness using Veritas, the object should be placed onto the x-y stage and measure the height of sample points on the surface of the object. Since the x-y stage could move along x and y axis in a perfect flat surface, it helps to keep away from the disturbance introduced by the measurement equipment.

Roundness of the print roller is targeted because of its critical impact towards the printing quality. Although the roundness of the print roller is very forgiving in self-assembly materials and the impression roller, which contacts the print roller during the printing process, could tolerate the variance of the roundness, the high roundness print roller is still desired in the view of future development. Because, if using some other materials that do not have self-assembly characteristics or very little pressure could be applied onto the print roller, a perfect roundness print roller is highly important to the final print quality.

In actual measurement, there is a problem with the roundness test due to the optical properties of PDMS. PDMS is an elastic transparent material that does not allow the laser sensor or the dial indicator to precisely measure the roundness variance. A few solutions could be applied to solve this issue: An interferometer is not limited by such kind of materials but it is too expensive for this project, or the stamp could be coated with metal powder and then use laser sensor to measure the distance, but this method will cause the damage of the stamp. Finally, the roundness of the printer roller could be indirectly indicated by the accumulate effect of the roundness of the print roller with the stainless steel sheet and the flatness of the stamp. The stamp is seamlessly attached to the stainless steel sheet; therefore, we assume the variance caused by the attachment is zero.

In the roundness test, since we are only interested in how round the print roller is when it is rolling for printing, and we are trying to compare the performance of different two wrapping systems, the measurement is taken separately in the two systems (i.e. that previous R2R system and updated R2R system detailed below) while simulating a real printing process. The final roundness information of the print roller is the aggregated result of the motor shaft eccentricity, motion transition quality of the connected bearings, roundness of the central shaft, roundness of the sleeve, variance caused by assembling the sleeve on the shaft, firmness of the attachment between the stainless steel sheet and the sleeve, and the flatness of the stamp. A dial indicator was used to make this measurement and figure 25 illustrates the general idea of the measurement settings.

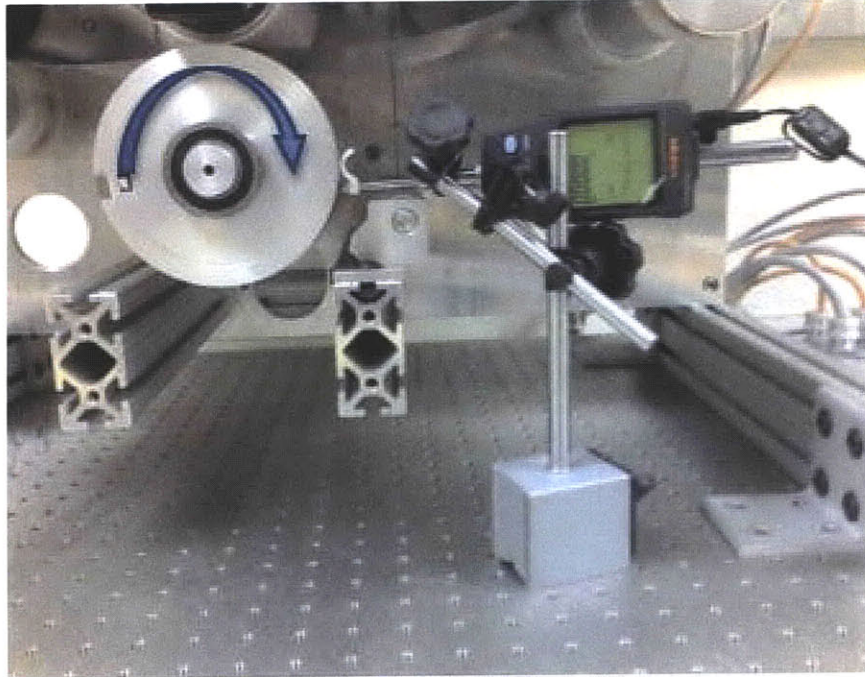


Figure 25: Measurement Setting for Roundness Measurement

With each rotation of the print roller, 16 sample points were collected at 3 positions along the roller (Front, Middle and Back), which means 16x3 sample points are collected for roundness analysis.

### 3.3.2 Distortion Measurement

After the features are successfully transferred from the stamp to the substrate (gold coated PET is the substrate used in this project), one of the most important quality indicators is the distortion of pixel on the substrate. The distortion is caused by several reasons:

1. Distortion of the flat stamp during the fabrication process
2. Distortion caused by wrapping the stamp onto the print roller
3. Tension in the substrate during printing
4. Deformation of the stamp from print pressure

All above sources of the distortion had been carefully analyzed in the thesis of *Analysis of the Capabilities of Continuous High-Speed Micro-contact Printing* <sup>[20]</sup> by Kanika Khanna. Based on her study, the wrapping process contributes the most to the final distortion.

The overall pattern printed comprises two types of pixel patterns, rectangular and triangular, as shown in Figs 28 and 29. . . The array of both of the these pixel patterns is shown in figure 30, where each pattern is printed on a 1.5mmx1.5mm square<sup>[20]</sup>.

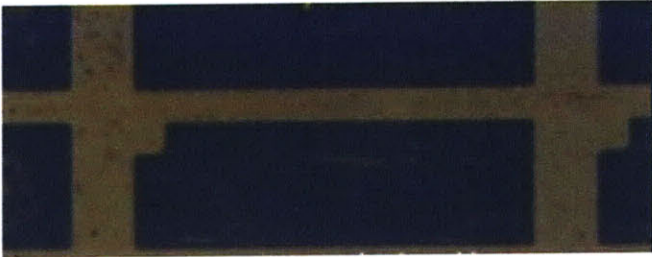


Figure 26: The Shape of Rectangular- like Pixel

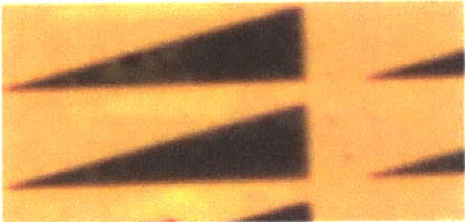


Figure 27: The Shape of Triangular Pixel

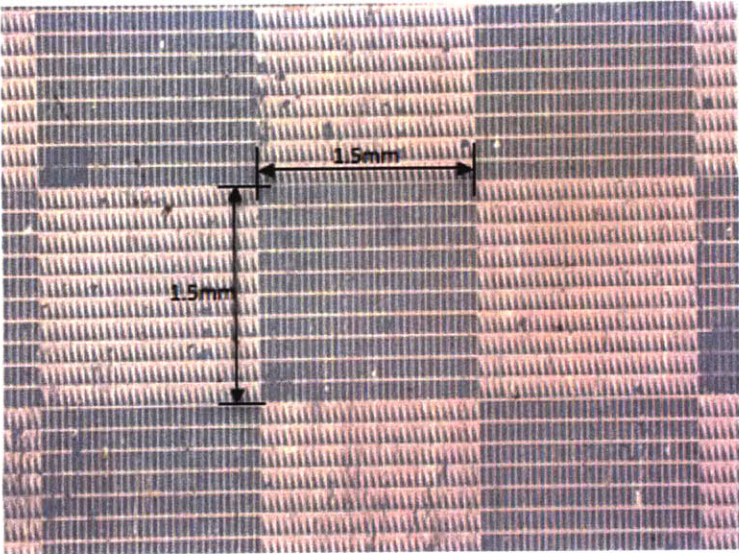


Figure 28: The Array of Two Kinds of Pixels

As mentioned before, the wrapping process causes distortion of the stainless steel sheet, which is used to hold the stamp in the printing process. The distortion of the stainless steel sheet leads to distortion of stamp, and hence the distortion of pixels.

Figure 31 demonstrates the distortion of pixel in a simply way. The black dashed rectangle is the standard shape of the pixel on the substrate and the blue solid rectangle is the distorted printed pixel. In figure 31, X and Y indicate the horizontal and vertical dimension of the standard pixel; X' and Y' indicate the corresponding dimension of printed pixel. It is important to note that the shape of distortion varies based on multiple reasons. To indicate the distortion, we will just simply use  $Y'/Y$  and  $X'/X$  as the distortion rate to identify the distortion over the Y and X axis

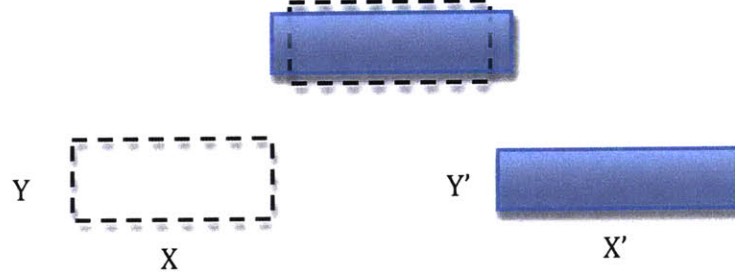


Figure 29: Demonstration of the Distortion

In order to make things easy, the distortion measurement is only taken on the rectangular-like pixels shown in figure 28, which is statistically representative to the overall distortion. For those rectangular-like pixels, their standard dimension is  $130\mu\text{m} \times 40\mu\text{m}$  AS shown in figure 32.

It is important to distinguish pixel distortion from pattern distortion. In this work we concentrate on distortions of at the pixel level, and are not concerned with overall pattern distortion caused by web movement or a non-parallel stamp on the roll. The stamp is made from a 300mm wafer, and the actual size of the square stamp is  $200\text{mm} \times 200\text{mm}$ . This area is evenly divided into  $5 \times 5$  cells with each cell being  $40\text{mm} \times 40\text{mm}$ . Within each cell, 5 pixels are randomly picked to measure, and averages to minimize the measurement error. This average is used to represent the dimension of the pixels in this area.

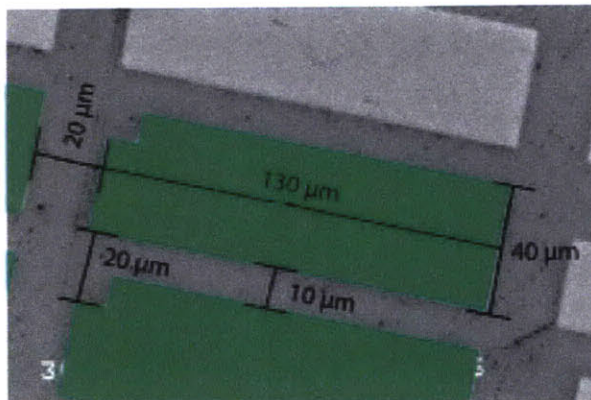


Figure 30: Pixel Dimensions [20]

### 3.3.3 Measurement of the Accuracy of the Alignment

The scope of the multi-layer printing in this project is to use the stamp to print twice on the same substrate without losing alignment. Therefore the accuracy of the alignment could be measured by indicating how well the overlap of two printed features, shown in Figure 31. In current stage, only x and y displacement are concerned. The angular misalignment is not included in the measurement due to the time constrain.

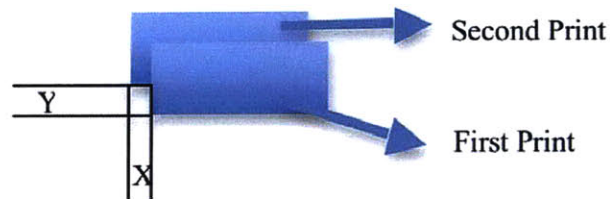


Figure 31: Displacement of Two Printed Layers

Same to the measurement of distortion, 5x5 matrix divided the 200mmx200mm printed area into 25 squares. Take the average of 4 measurement within each square for the x and y displacement.

## **4 The Wrapping Problem**

### **4.1 Overall Goal**

The MIT '08 project achieved 100% pattern transfer on to the substrate at a speed of 400 feet per minute using microcontact printing. The emphasis was on speed, with quality as a secondary objective, almost considered a bonus. In short, the '08 project proved that microcontact printing on a roll-to-roll paradigm could be an industry-competitive solution with regards to the speed of printing. An obvious progression of this experiment was proving that the quality of printing achieved via microcontact printing would also match, if not surpass, that of competitive technologies. Thus, the '09 project was concerned with making the MIT '08 roll-to-roll machine, high precision, and maximizing the quality of the print output. This section focuses on the improvement of a particular process that directly influences the print quality, namely, the process of wrapping the elastomeric stamp on the print roller.

### **4.2 The Existing Wrapping Process**

Roll-to-roll equipment was designed and built in the MIT 08 project. The wrapping process consisted of two separate steps:

- Peeling the PDMS stamp on the backing plate off the Silicon wafer
- Wrapping the backing plate and stamp on the print roller

However, this process had three major shortcomings:

1. **Manual Handling:** The wrapping step, involved a lot of manual handling that risked causing damage to the backing plate by introducing wrinkles, or other irregularities on the geometry
2. **Lack of Alignment:** The backing plate was wrapped on the roller by clamping its ends into a groove in a retainer bar (Figure 32). This system of attachment did not guarantee any particular level or repeatability, or precision.

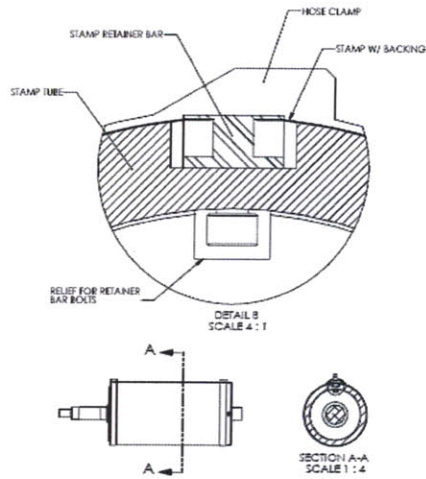


Figure 32: A section view of the existing stamp-roller interface [4]

3. Lack of Force of Attraction: The material of the old print roller was aluminum. Thus, there is no force of attraction on the curved surface of the cylinder to pull the backing plate to it. This resulted in air gaps, or even large visible bumps of the backing plate on the roller. One such bump is shown in Figure 33.

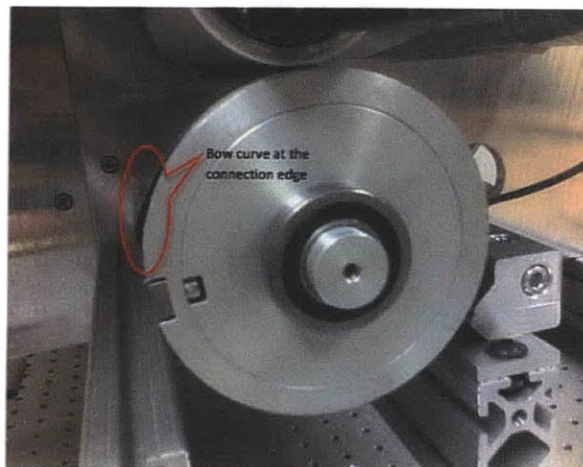


Figure 33: This figure shows a significant air gap between the print roller and the backing plate from the MIT '08 configuration

### **4.3 Requirements of Proposed Wrapping System:**

The new system must eliminate the problems with the '08 system, while also enabling the fulfillment of the goals of the project.

Thus, in order to overcome the shortcomings with the existing wrapping system, we decided to combine the two steps involved – peeling and wrapping. This would eliminate all problems that stem from manual handling, thus preserving original stamp quality, and hence printing quality.

To overcome the second shortcoming, that of repeatability and precision of alignment of the backing plate with the print roller, we decided to use two precision dowel pins as a means to establish and maintain precise alignment during the wrapping process.

And, finally, to overcome the third shortcoming, the print roller must exert a uniform attraction force throughout its curved surface area, on maximum are of the backing plate.

Hence, functional requirements of the wrapping system are:

1. Peel PDMS stamp off the Silicon wafer
2. Wrap the PDMS stamp with the stainless steel backing plate on the print roller without air gaps
3. Maintain alignment of the stamp with the print roller during steps 1 and 2
4. Enable compatibility with the precision positioning system (the precision positioning system is described in detail in Paolo Baldesi's thesis [25])

### **4.4 The Peeling Process Design:**

As introduced, the peeling process must ensure that the backing plate along with the PDMS stamp separates from the Silicon wafer. The crucial question addressed in this design was how to simultaneously achieve the peeling of the backing plate and PDMS stamp from the Si wafer, and the wrapping of the same on the magnetic cylinder, while maintaining alignment.

The print roller must have the capability of combining these two steps into a continuous movement. Hence, alignment of the backing plate with the print roller must be achieved during the peeling step itself, as there is no subsequent wrapping step to establish or



alter alignment between the two. Thus, the first contact between the magnetic sleeve and the backing plate must first define alignment with high-precision, and then initiate peeling.

## **4.5 Design of Mechanics of First Contact**

### **4.5.1 Alignment Mechanism**

As described above, the initial alignment of the roller with the backing plate would define the precision of the rolling, and the quality of the print output. Thus, this alignment is a critical part of the wrapping process. We chose a pin-hole and pin-slot combination as the means of this alignment, i.e. the print roller will have two precision holes with two dowel pins (slide fit) and these pins will mate with a corresponding hole and slot in the backing plate to establish alignment. The precision of this alignment will be defined by the clearance between the dowel pins and the hole (and slot).

### **4.5.2 Sources of Error during Alignment**

#### **1. Error in size of backing plate**

Based on the budget available, and a suitable manufacturing process to cut the backing plate (laser cutting), this error in size is given by the following tolerances:

Width = 230 mm  $\pm$  2.5 microns  
Length = 320 mm  $\pm$  2.5 microns

#### **2. Clearance between pins and holes**

This clearance depends on the tolerances on the dimensions of the pins and the holes. Assuming the worst case, i.e. the maximum clearance between pin and hole. This will occur at smallest pin size, and biggest hole size. According to pin and hole specifications,

Tolerances:

Pin: 0.125"  $\pm$  0.0001"  
Hole/Slot: 0.1255"  $\pm$  0.0005"

Thus, in the worst case,

Pin diameter: 0.1249"

Hole/slot size: 0.126"

$$\begin{aligned}\text{Total Clearance} &= 0.126'' - 0.1249'' \\ &= 0.0011'' \\ &= 27.94 \text{ microns}\end{aligned}$$

Due to this clearance between the pins and the holes, there will be two types of errors

#### 1. Lateral Error

This error will be due to the possibility of lateral movement of the backing plate with respect to the pins. The maximum lateral error will equal to the total clearance between the pins and holes, and is given by,

$$\text{Lateral Error} = 27.94 \text{ microns}$$

## 2. Angular Error

This error will be result of pivoting of the backing plate about the two pins, once again due to the clearance between the pins and holes. The angular error is calculated as shown in figure 34.

$$\begin{aligned}
 \text{Error Angle} &= \tan^{-1} (\text{Clearance} / \text{Distance}) \\
 &= \tan^{-1} (27.94 \text{ microns} / 220 \text{ mm}) \\
 &= 7.277 \times 10^{-3} \text{ degrees}
 \end{aligned}$$

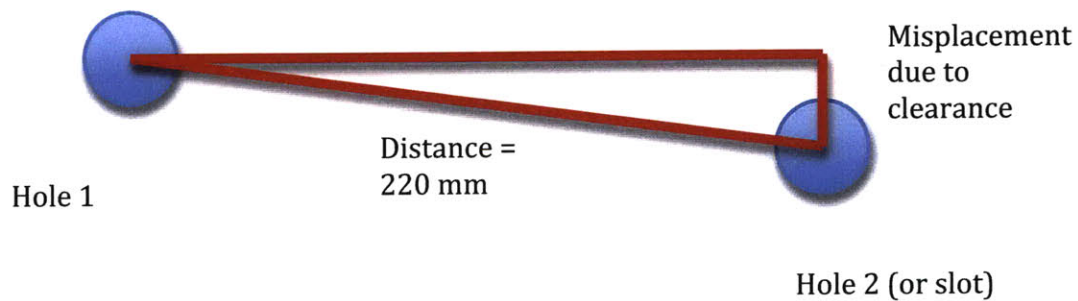


Figure 34: Shows calculation of error angle due to clearance between pins and holes

As shown in Figure 35 below, due to this error angle, there will be a lateral displacement, given by

$$\begin{aligned}
 \text{Angular Error} &= \text{Length of plate} \quad \times \quad \sin (\text{Error Ang.}) \\
 &= 320 \text{ mm} \quad \times \quad \sin (7.277 \times 10^{-3} \text{ deg}) \\
 \text{Angular Error} &= \quad \mathbf{41 \text{ microns}}
 \end{aligned}$$

Thus, total clearance error,

$$\begin{aligned}
 \text{Total Error} &= \text{Lateral Error} \quad + \quad \text{Angular Error} \\
 &= 27.94 \text{ microns} + \quad 41 \text{ microns} \\
 \text{Total Clearance Error} &= \quad \mathbf{68.94 \text{ microns}}
 \end{aligned}$$

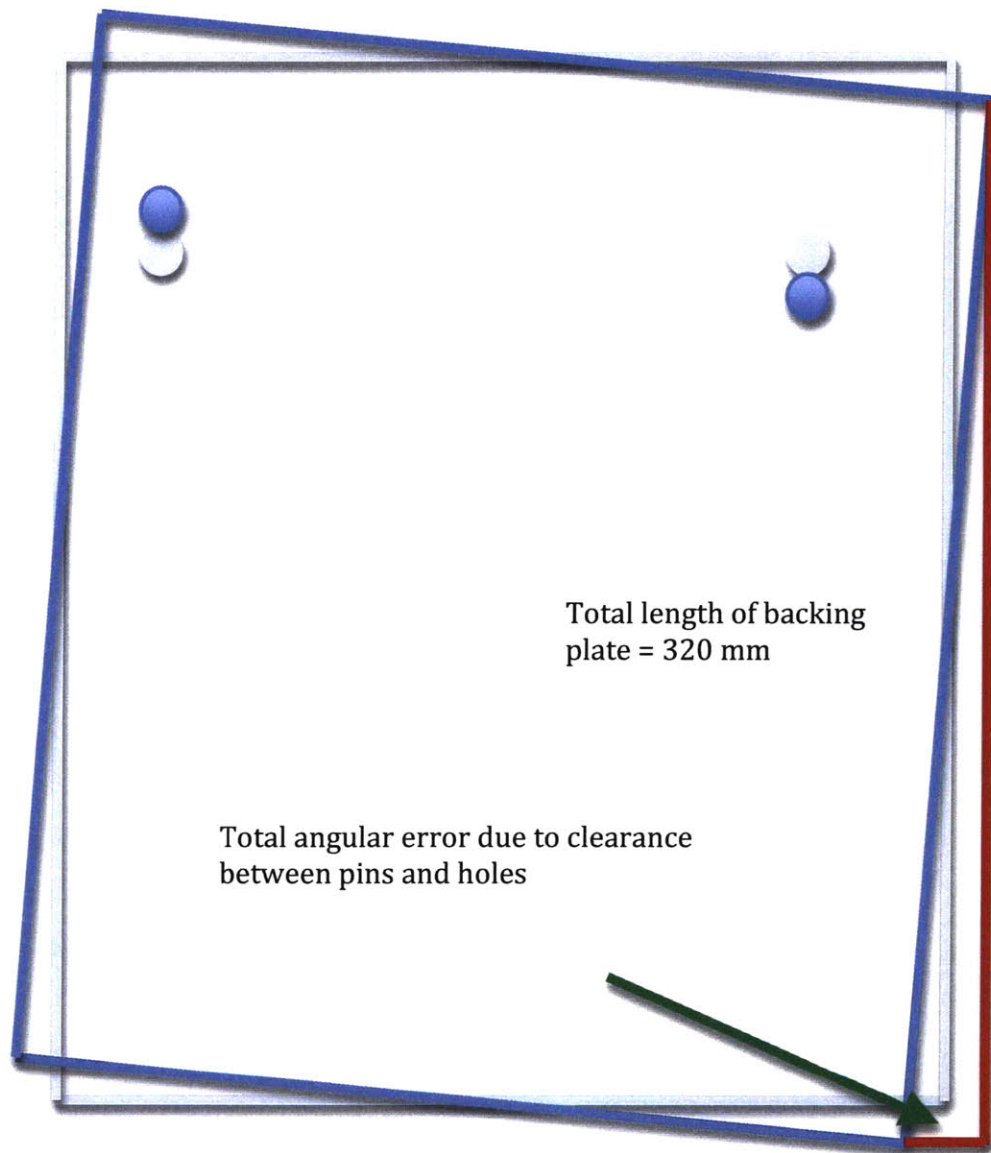


Figure 35: Gray: Ideal position of backing plate, Blue: Rotated position of backing plate due to clearance between holes and pins, Red: Angular Error

### 4.5.3 Alignment Process

The initial pre-peeling setup is as shown below (Figure 36).

The print roller must be brought close to the backing plate manually. Next, alignment pins that are inserted in the corresponding holes in the print roller will be used to establish alignment between the roller and the backing plate. Inserting the alignment pins into corresponding holes in the backing plate will do this.

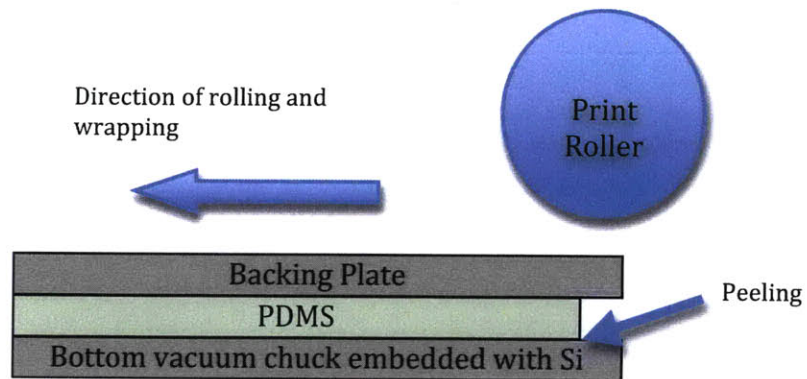


Figure 36: Illustration of setup before wrapping

Once this alignment is established, the next step is to peel the backing plate attached to the PDMS stamp, while maintaining alignment, and to wrap the backing plate onto the print roller.

Upon wrapping the backing plate on the roller, it must be ensured that the backing plate does not move relative to the print roller.

## 5 Design

This design problem can be divided into two parts:

- Wrapping system
- Mounting of the print roller onto the MIT '08 machine

We first consider the design of the wrapping system

### 5.1 Wrapping System

This system is concerned with the attachment of the backing plate to the print roller. The mechanics of the peeling-wrapping process are discussed along with their influence on the design of the components of the wrapping system.

#### 5.1.1 Concept Selection

**Attachment:** As described in the Methodology section, several methods of attaching the backing plate to the print roller were considered before magnetism was chosen as the best one.

**Alignment:** During the peeling-wrapping process, the first contact will establish and define alignment between the print roller and the backing plate. In order to ensure minimal distortion of the PDMS while wrapping, this alignment must be precise. A pin and hole type of alignment method was chosen because the error in this system is only the clearance between the pins and the holes. Choosing high-precision dowel pins, and precision manufacturing operations to machine the hole and slot can minimize this error. As seen in section 4.5.2, this error can be easily controlled to less than 100 microns.

### 5.1.2 Experiments to Simulate the Peeling-Wrapping Process:

Upon selecting the method of establishing attachment and alignment between the print roller and the backing plate, next it was necessary to conduct simple experiments to assess the nature of these problems, and to make preliminary assumptions and preliminary design choices. Several simple experiments using double-sided tape (as a substitute for magnetic strips) were conducted to estimate if the new peeling-wrapping process was a practical solution. Two significant experiments are described below.

### 5.1.3 Experiment #1: Simulation of the new peeling-wrapping process.

For this experiment, an aluminum shaft was machined, using the dimensions of the MIT '08 print roller. Next, holes were drilled in the cylinder, and several dowel pins of diameter 3 mm were press fit in these holes. These pins protruded less than 1 mm from the surface of the cylinder. Next, double-sided tape was applied to the upper surface of the cylinder, to simulate a magnetic force of attraction. Also, a stainless steel sheet (backing plate) of 0.005" thickness was cut to suitable dimensions for wrapping it on the shaft. Two holes corresponding to the pins in the cylinder were punched in the backing plate. Next, a flat stamp was cast using the 6" wafer chuck.

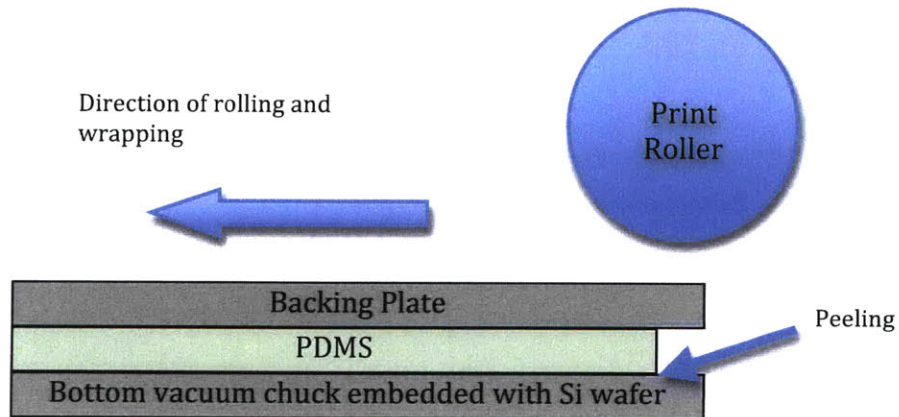


Figure 37: Illustration of setup before wrapping

As shown in figure 37, the print roller was brought close to the backing plate with the stamp underneath it. Then the pins in the roller were aligned with corresponding punched holes in the backing plate. Next, the new peeling-wrapping process was conducted, by manually rolling the shaft over the backing plate, and peeling and wrapping the backing plate successfully. This was the first experiment where the combined peeling-wrapping process was simulated.

#### 5.1.4 Results:

1. Firstly, successful peeling can be defined as tear-free peeling of the PDMS stamp off the Silicon wafer. Also, another important factor to consider is damage or deformation of PDMS due to the weight of the roller bearing down on it during wrapping. Since the wrapping process is manual, it is up to the skill of the operator to ensure that he/she does not let all the weight of the roller transfer onto the PDMS and the Si wafer.  
The peeling process was not successful, because, a part of the PDMS stamp was torn off. However, this was attributed a fault during the casting of the stamp. Thus, the cause of this problem was not the peeling process itself.  
Also, there was no deformation of the PDMS.
2. Also, the stamp did not tear after it was wrapped on the roller.
3. The alignment of the backing plate on the cylinder was also a simple, and precise method, proving that the pin and hole alignment mechanism would work.

This experiment helped conclude the following:

This experiment provided first-hand information about the force required to peel the PDMS stamp off the Silicon wafer, The force was not measured, but was found to be low enough to allow easy peeling without tearing or excessive stressing of the backing sheet. Also, since the adhesive force from the double-sided tape was found to be sufficient to provide this peeling force; much larger magnetic force provided by a magnetic roll would prove even more effective for the peeling process.

The pin and hole alignment method was found to be effective. This method ensured a repeatable position of the backing plate on the roller, upon completion of wrapping. In fact, the wrapping process was conducted 10 times, and the process was found to be repeatable to within 1 mm (using crude measurement techniques). This method lowered the sources of error to only errors of position and size of the backing plate and the hole and the slot in it.

The 0.005" thick backing plate was easy to accurately wrap on the roller with the help of a small, yet well-distributed attractive force. This proved that the initial alignment using pins-holes was responsible for repeatable wrapping, without the need of a guiding system. The repeatability of the wrapping process is because the backing plate is a rigid material in the lateral direction (perpendicular to the wrapping direction), and thus does not distort or twist even in the absence of a guiding system. In fact, the use of a guiding system would over constrain the rigid backing plate in the lateral direction, and would develop stresses in the plate resulting in undesirable distortions and wrinkles on the



surface of the backing plate. Thus, upon wrapping the backing plate on the roller, these distortions would have an adverse effect on the print output.

This experiment enabled several design decisions, one of which was to use of magnetism as the primary source of attraction force between the print roller and backing plate.

Following this, it was necessary to decide whether such a magnetic cylinder needed to be custom-manufactured, or an adaptable industry solution existed. After research into the printing, and allied industries, it was discovered that the die-cutting (and hot embossing) industry does make use of patented magnetic cylinders. These consist of an array of magnetic strips made of rare-earth permanent magnet blocks (Figure 38 [35]) that could be used for our printing application.

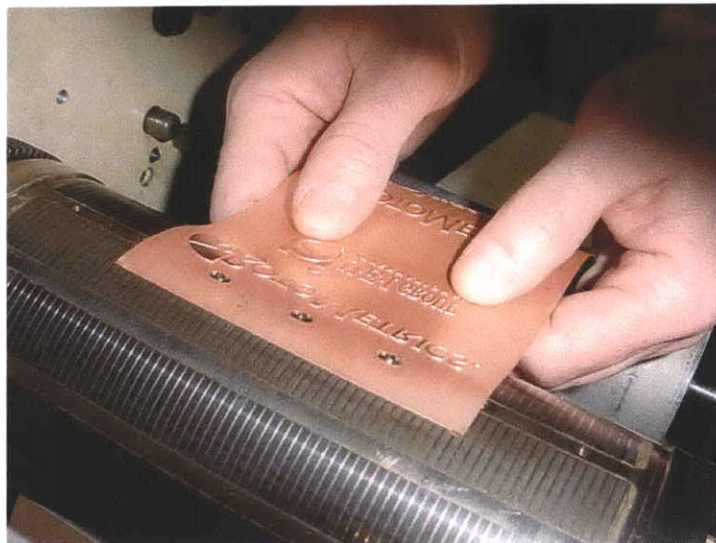


Figure 38: Shows the magnetic strips on the magnetic cylinder, and its conventional application in the die-cutting industry. The flexible plate being attached to the cylinder is patterned. [35]

### 5.1.5 Wrapping Demonstration with Sample Magnetic Cylinder and Backing Plate:

As shown in figure 38, a demonstration was conducted by Ed Miklos, Rotometrics, at Nano Terra,, where a steel backing plate was manually wrapped around a sample magnetic cylinder.

The following observations were made:

The magnetic force is strong. The backing plate sticks to the magnet strips if brought to a distance less than 5 mm from the surface of the magnet strip.

Two higher strength magnet strips will be needed to tightly clamp both the edges of the backing plate to the magnetic sleeve

#### Conclusion:

**Maneuverability During First Contact:** During the first contact, while aligning the pins of the print roller, with the holes in the backing plate, a force of attraction as strong as that exerted by the magnetic strips, is highly undesirable, and could cause premature peeling of the backing plate and stamp from the wafer, rendering the stamp useless. Thus, sufficient area in the vicinity of the alignment pins on the print roller must be non-magnetic.

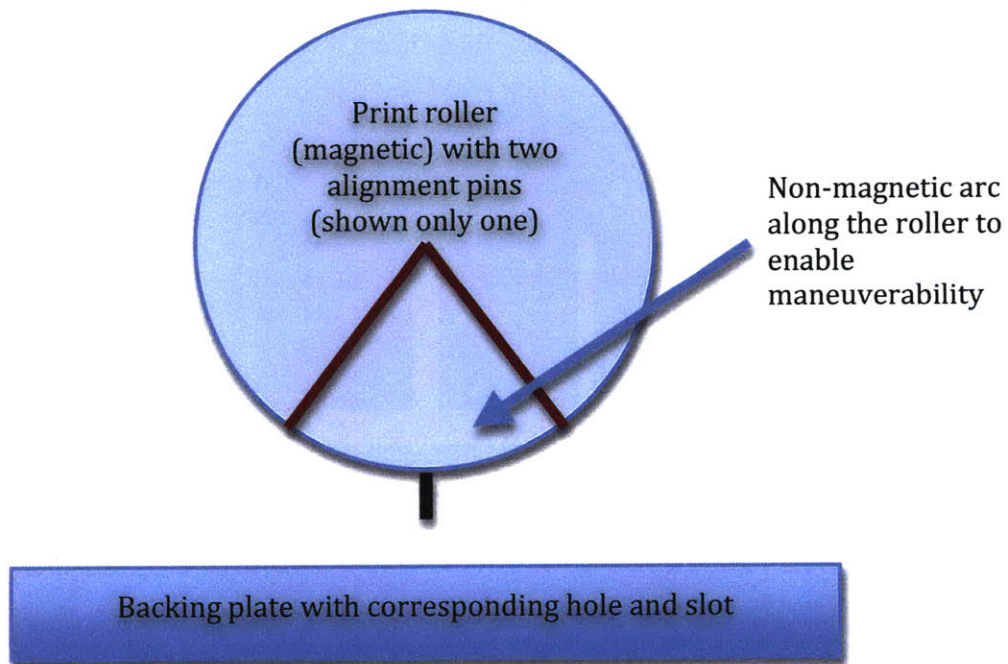


Figure 39: The non-magnetic arc in the print roller

### 5.1.6 Design of Print Roller

The print roller consists of a large number of magnetic strips, covering an area equal to the length of the backing plate, 320 mm. The spacing of the magnetic strips on the magnetic cylinder was decided taking into account the results of the demonstration described above. An experiment was conducted using an Aluminum cylinder equal in diameter to the print roller, to estimate the dimensions of the non-magnetic area needed around the alignment pins.

#### Non-Magnetic Area:

Based on the data provided by the magnetic cylinder manufacturing company (Rotometrics [38] – a manufacturer of precision rotary tooling), and based on the demonstrations and experiments we conducted, approximately 15 mm distance between the magnetic strip on the cylinder and the backing plate would be needed to preclude the possibility of accidental attachment of the backing plate to the magnetic cylinder. Avoiding this accidental attachment is critical in avoiding tearing of the stamp.

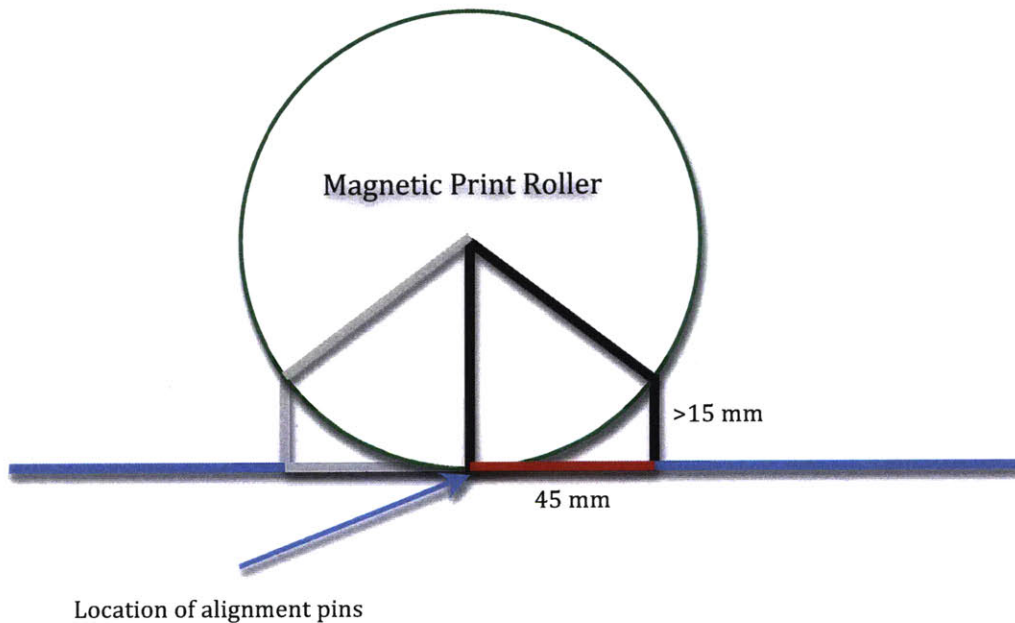


Figure 40: Illustration showing non-magnetic area on the print roller

It was calculated that an arc of close to 45 degrees on either side of the alignment pins of the print roller must be non-magnetic.

As shown in figure 41, the backing plate covers approximately 292 degrees on the circumference of the print roller. Of this, the yellow part shows the non-magnetic region that enables maneuverability of the print roller during the pre-peeling alignment setup.

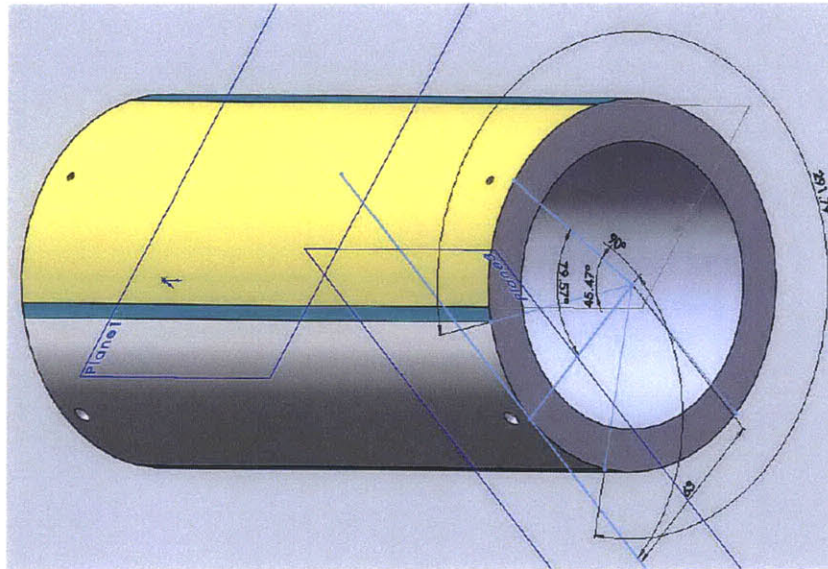


Figure 41: Illustration of the print roller; Yellow: non-magnetic area for the peeling-wrapping process. Gray: Area not covered by backing plate, hence non-magnetic. Teal: Magnetic strips (not to scale)

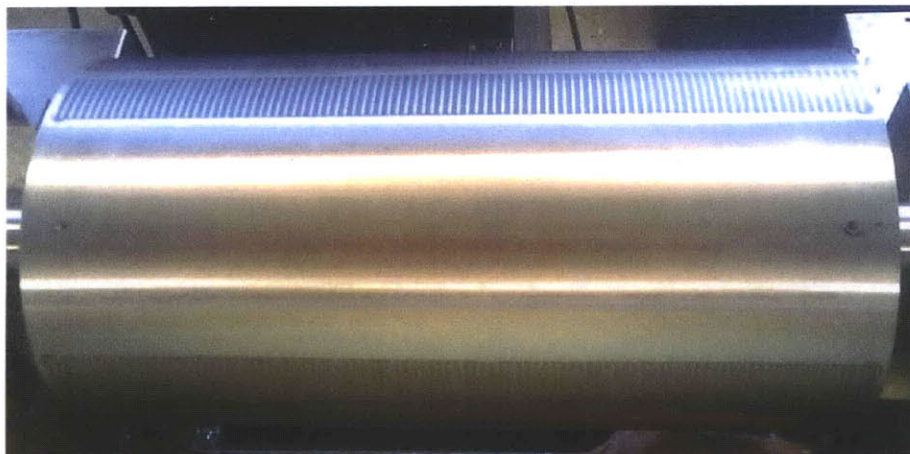


Figure 42: Photo of Final Roll Provided by Rotometrics, showing the non magnetic part of sleeve

### **5.1.7 Design of Backing Plate**

The backing plate basically lends rigidity to the otherwise flexible PDMS stamp. Hence, a metallic backing plate is chosen as a support for the PDMS. Since magnetism is chosen as the method to attach the backing plate to the print roller, the material of the backing plate must be magnetic.

Successful peeling consists of the following:

1. The PDMS stamp peels off from the Silicon wafer
2. The PDMS stamp remains uniformly and fully attached to the backing plate
3. The PDMS does not deform or compress due to weight of the roller
4. The backing plate attaches uniformly and fully to the print roller

Thus, the force of attraction between the PDMS and the backing plate must be greater than the force of attraction between the PDMS and the Silicon wafer. The surface of the backing plate is subject to corona treatment for this purpose. Hence, one of the important requirements of the material of the backing plate is the compatibility to this treatment. Stainless steel is one such compatible material. Keeping this in mind, a magnetic grade of stainless steel was chosen for the backing plate.

Material Selected: 410 Annealed Stainless Steel

#### **To find optimum position of alignment holes on backing plate:**

Based on the experiments conducted to establish alignment of the print roller to the backing plate prior to the peeling-wrapping process, it was determined that 45 degrees on either side of the alignment pins on the print roller must be non-magnetic.

In addition to this requirement, the weight of the print roller was also seen as an important factor during the initial alignment process. As shown in the configuration below, the PDMS stamp is sandwiched between the backing plate and the vacuum chuck. In order to avoid compression of the PDMS, the weight of the print roller should not, at any point, bear down on the PDMS.

Thus, taking these two factors into consideration, the alignment hole and slot are located at least 50 mm away from the edge of the stamp. As shown in figure 43, the print roller, during the alignment process, bears down on that part of the backing plate below which is the rigid Teflon ring, and not that part which covers the PDMS.

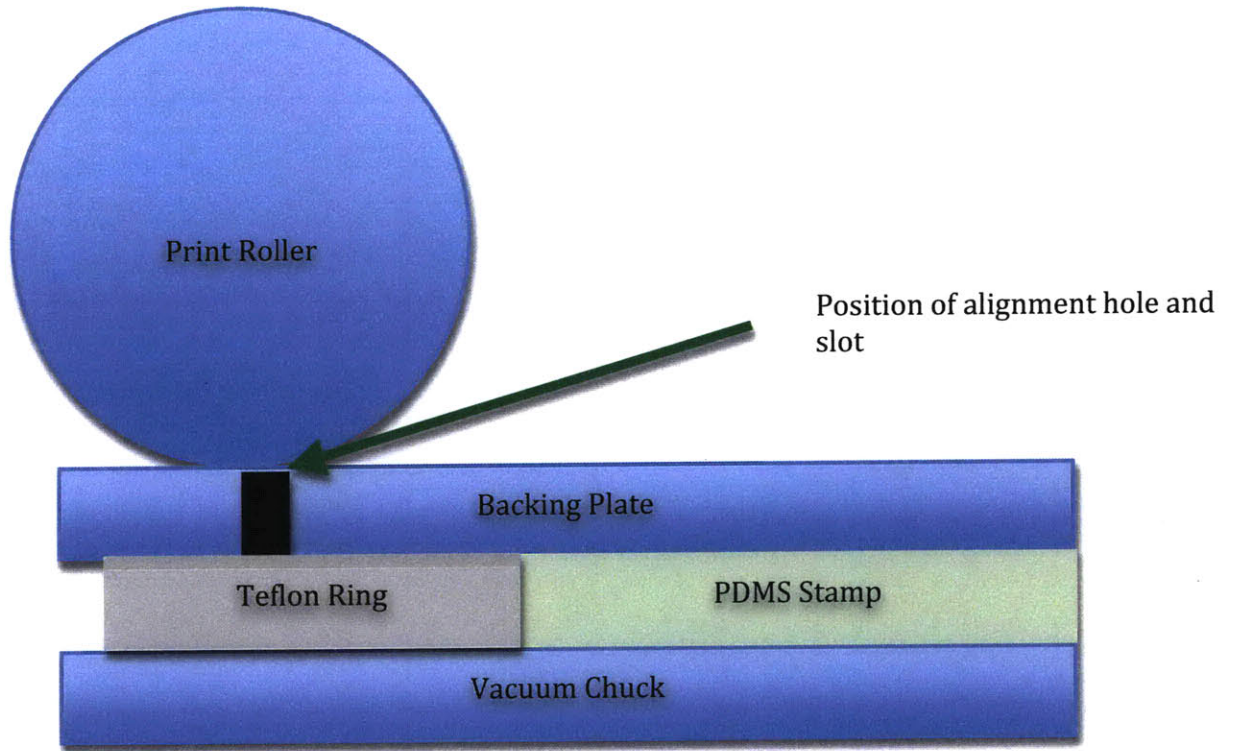


Figure 43: Determination of the position of alignment hole and slot in backing plate (illustration not to scale)

### Strain: Elongation Calculation [33]

The flat PDMS stamp must be wrapped onto the cylindrical print roller. Upon wrapping, the stamp material will be slightly stretched as result of bending. This elongation is an important metric in finding out the effect of wrapping on the size of the features to be printed. If this elongation is significant, i.e. if the features deform considerably due to wrapping, their original shape (before wrapping) must be designed keeping this elongation in mind.

Using theory of bending of beams, we know that, strain during bending is given by:

$$\epsilon = \frac{r}{R} \quad (\text{Eq. 1})$$

where the terms are defined in Fig. 44

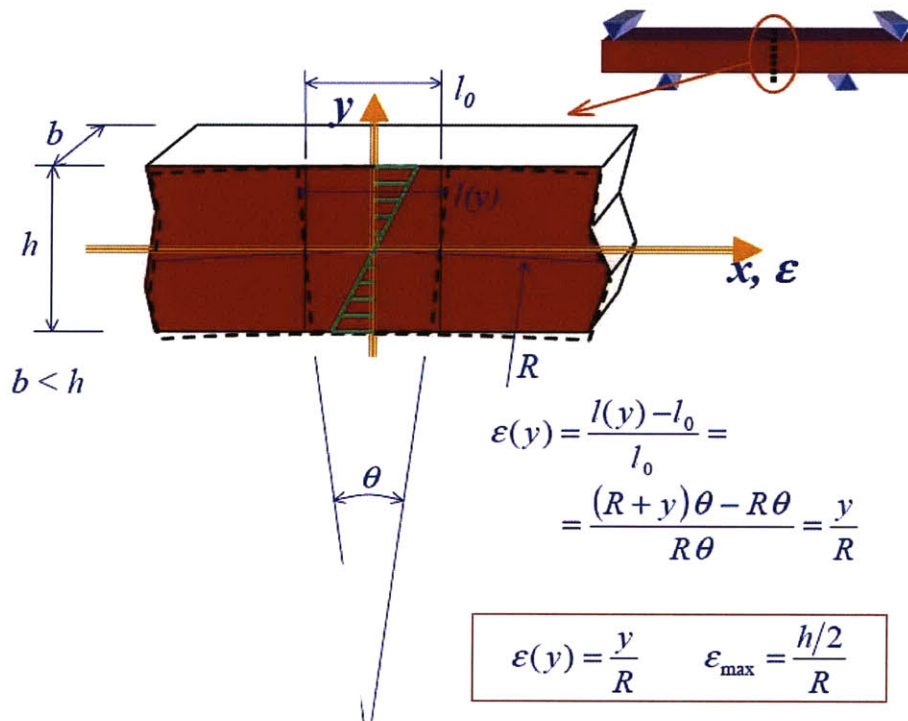


Figure 44: Derivation of strain elongation in beams subjected to pure moment bending. This is equivalent constant radius deformation as is the case here [33]

In our case, we want to calculate elongation of the PDMS stamp.

In order to simplify, we make one basic assumption, that the backing plate has a negligible thickness (0.127 mm), and hence, the backing plate is neglected in this analysis.

Thus,

$$\begin{aligned} R &= \text{radius of print roller} + (\text{thickness of PDMS})/2 \\ &= 63 \text{ mm} + (0.800)/2 \text{ mm} \\ R &= 63.400 \text{ mm} \end{aligned}$$

Also,

$$\begin{aligned} r &= (\text{Thickness of PDMS}) / 2 \\ &= 0.400 \text{ mm} \end{aligned}$$

$$\text{Thus, } \varepsilon = \frac{0.4}{63.4} = 0.63\%$$

Consider a feature (like a pixel) on the patterned PDMS stamp, is a square of 40 x 40 microns.

This means that along the 40-micron length of the feature, there will be an elongation of

$$\varepsilon_{\text{feature}} = \frac{0.0063\text{mm}}{0.040\text{mm}} = 0.25\text{microns}$$

This information can be used when designing the size of the features on the PDMS stamp, to compensate for this error due to wrapping.



## 5.2 Mounting of the Print Roller onto the MIT '08 Machine

The print roller must be mounted on the existing equipment. However, a new Precision Positioning System has been designed.

This system allows adjustment of the position of the print roller about five degrees of freedom. Thus, the mounting system, and each of its components, has been designed so as to allow all these fine adjustments.

For details of the Precision Positioning System, the reader is referred to Paolo Baldesi's thesis [25].

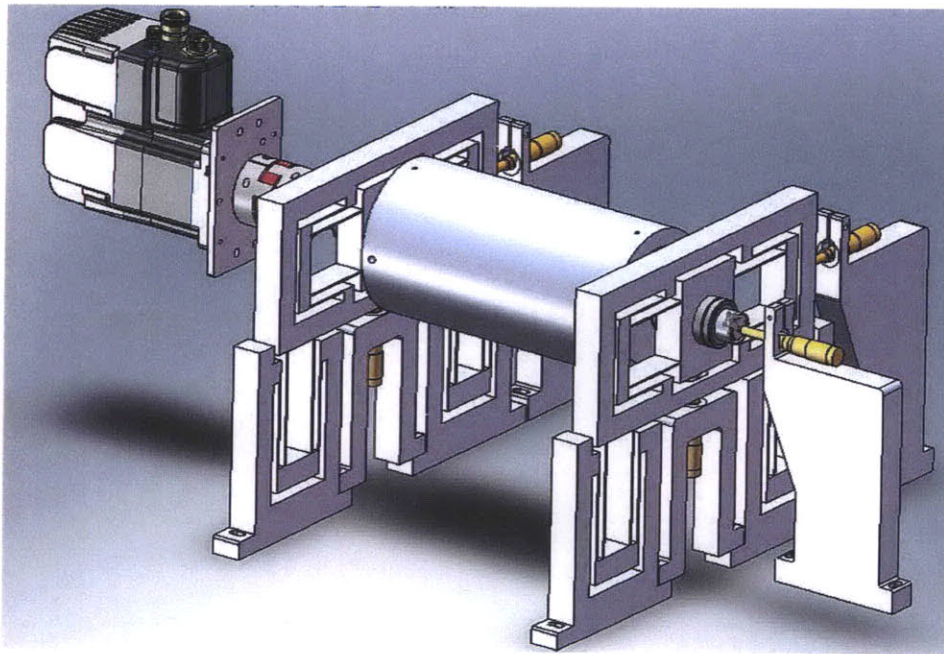


Figure 45: CAD model of the new print roller mounted on the Precision Positioning System [1]

In the existing equipment, the print roller is connected to a driving motor via a flexible coupling. However, there is no means for adjusting the position of the print roller. The connection between the motor and the print roller must enable this adjustment. Hence, this connection, or coupling, must be of a repeatable, flexible nature.

### 5.2.1 Flexible Coupling Design

The coupling connects the shaft to the driving motor. Note that the motor is fixed to the frame of the machine, whereas the sleeve-shaft system must be adjustable about 5 axes. This is accomplished via the coupling. Hence, The coupling has to fulfill certain requirements in terms of the range of adjustment it allows, enabling the working of the Precision Positioning System. This means that the coupling must allow certain minimum misalignments, as follows:

Lateral Misalignment (mm):	0.12
Angular Misalignment (Degree):	1.0
Axial Misalignment (mm):	1.5

The combination of these misalignments satisfies the requirements of the Precision Positioning System.

#### 5.2.1.1 Calculations and Selection [31]

We first calculate the minimum torsional stiffness of the coupling.

$$C_T \geq \frac{(F_R \times 2\pi)^2}{\left(\frac{1}{J_M} + \frac{1}{J_L}\right)} \quad (\text{Eq. 2})$$

Where,

CT = torsional stiffness (Nm/rad)  
JM = motor inertia (kgm<sup>2</sup>) = 4.8 x 10<sup>-7</sup> kgm<sup>2</sup>  
FR = resonant frequency (Hz)

$$= \frac{1}{2\pi} \times \sqrt{\frac{nT}{I}} \quad (\text{Eq. 3})$$

Where, n = number of poles of motor = 2

T = holding torque = 12.07 Nm

I = motor inertia = 4.8 x 10<sup>-7</sup> kgm<sup>2</sup>

FR = 1128.67 Hz

$$\begin{aligned}
 JL &= \text{load inertia (kgm}^2\text{)} \\
 &= \frac{20\text{kg} \times (0.063\text{m})^2}{2} \\
 &= 0.05 \text{ kgm}^2
 \end{aligned}$$

Thus,  $CT \geq 24.14 \text{ Nm/rad}$

### 5.2.1.2 Flexibility Requirements:

Lateral Misalignment (mm): 0.12  
 Angular Misalignment (Degree): 1.0  
 Axial Misalignment (mm): 1.5

Table 1: Coupling Selection [32]

Model EK	Coupling series (2 - 60)																																																											
	2			5			10			20			60																																															
Type (Elastomer insert)	A	B	C	A	B	C	A	B	C	A	B	C	A	B	C																																													
Static Torsional stiffness (Nm/rad)	<div style="display: flex; align-items: center;"> <div style="writing-mode: vertical-rl; transform: rotate(180deg); font-weight: bold; margin-right: 5px;">CT</div> <table border="1"> <tr> <td>5</td><td>1</td><td>1</td> <td>1</td><td>3</td><td></td> <td>2</td><td>60</td><td>90</td> <td>11</td><td>25</td><td>52</td> <td>32</td><td>975</td><td>1400</td> </tr> <tr> <td>0</td><td>5</td><td>7</td> <td>0</td><td>0</td><td>53</td> <td>6</td><td>0</td><td></td> <td>40</td><td>00</td><td>0</td> <td>90</td><td>0</td><td></td> </tr> </table> </div>															5	1	1	1	3		2	60	90	11	25	52	32	975	1400	0	5	7	0	0	53	6	0		40	00	0	90	0																
5																1	1	1	3		2	60	90	11	25	52	32	975	1400																															
0	5	7	0	0	53	6	0		40	00	0	90	0																																															
Dynamic Torsional stiffness (Nm/rad)	<div style="display: flex; align-items: center;"> <div style="writing-mode: vertical-rl; transform: rotate(180deg); font-weight: bold; margin-right: 5px;">CTdyn</div> <table border="1"> <tr> <td>1</td><td>2</td><td>3</td> <td>3</td><td>7</td><td>10</td> <td>5</td><td>16</td><td>22</td> <td>25</td><td>44</td><td>87</td> <td>79</td><td>119</td><td>1350</td> </tr> <tr> <td>0</td><td>3</td><td>5</td> <td>0</td><td>0</td><td>6</td> <td>4</td><td>50</td><td>4</td> <td>40</td><td>40</td><td>6</td> <td>40</td><td>00</td><td></td> </tr> <tr> <td>0</td><td>0</td><td></td> <td>0</td><td>0</td><td></td> <td>1</td><td></td><td></td> <td></td><td></td><td></td> <td></td><td></td><td></td> </tr> </table> </div>															1	2	3	3	7	10	5	16	22	25	44	87	79	119	1350	0	3	5	0	0	6	4	50	4	40	40	6	40	00		0	0		0	0		1								
1	2	3	3	7	10	5	16	22	25	44	87	79	119	1350																																														
0	3	5	0	0	6	4	50	4	40	40	6	40	00																																															
0	0		0	0		1																																																						
Lateral (mm)	<div style="display: flex; align-items: center;"> <div style="writing-mode: vertical-rl; transform: rotate(180deg); font-weight: bold; margin-right: 5px;">Max. values</div> <table border="1"> <tr> <td>0,0</td><td>0,0</td><td>0,0</td> <td>0,0</td><td>0,0</td><td>0,0</td> <td>0,0</td><td>0,08</td><td>0,1</td> <td>0,1</td><td>0,08</td><td>0,1</td> <td>0,12</td><td>0,1</td><td>0,15</td> </tr> <tr> <td>8</td><td>6</td><td>1</td> <td>8</td><td>6</td><td>1</td> <td>1</td><td></td><td></td> <td></td><td></td><td></td> <td></td><td></td><td></td> </tr> </table> </div>															0,0	0,0	0,0	0,0	0,0	0,0	0,0	0,08	0,1	0,1	0,08	0,1	0,12	0,1	0,15	8	6	1	8	6	1	1																							
0,0	0,0	0,0	0,0	0,0	0,0	0,0	0,08	0,1	0,1	0,08	0,1	0,12	0,1	0,15																																														
8	6	1	8	6	1	1																																																						
Angular (degree)	<div style="display: flex; align-items: center;"> <table border="1"> <tr> <td>1</td><td>0,8</td><td>1,2</td> <td>1</td><td>0,8</td><td>1,2</td> <td>1</td><td>0,8</td><td>1,2</td> <td>1</td><td>0,8</td><td>1,2</td> <td>1</td><td>0,8</td><td>1,2</td> </tr> <tr> <td>8</td><td>2</td><td></td> <td>8</td><td>2</td><td></td> <td>8</td><td></td><td></td> <td>8</td><td></td><td></td> <td>8</td><td></td><td></td> </tr> </table> </div>															1	0,8	1,2	1	0,8	1,2	1	0,8	1,2	1	0,8	1,2	1	0,8	1,2	8	2		8	2		8			8			8																	
1	0,8	1,2	1	0,8	1,2	1	0,8	1,2	1	0,8	1,2	1	0,8	1,2																																														
8	2		8	2		8			8			8																																																
Axial (mm)	<div style="display: flex; align-items: center;"> <table border="1"> <tr> <td>±1</td><td></td><td></td> <td>±1</td><td></td><td></td> <td>±1</td><td></td><td></td> <td>±2</td><td></td><td></td> <td>±2</td><td></td><td></td> </tr> </table> </div>															±1			±1			±1			±2			±2																																
±1			±1			±1			±2			±2																																																

Selected Coupling: The Model EK Series 60, Type "C" coupling satisfies all the requirements.

Features [30]:

- Zero backlash error
- Robust

The flexible coupling thus allows micro adjustments about the five axes, enabling the Precision Positioning System. However, micrometer heads will bring forth these adjustments.

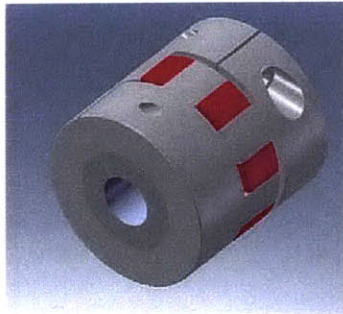


Figure 46: Shows the chosen Flexible Coupling [39]

### **5.2.2 Design to Enable X-Axis Positioning**

The main requirement of this system is to adjust the position of the magnetic sleeve with respect to the web along the X-axis. This is a translational adjustment. The flexible coupling does permit this adjustment. However, we also considered using a compression spring, as an additional component to make this adjustment easier.

Thus, two concepts were proposed, one using a compression spring along with a lead screw for adjustment, and the other, using flexible coupling along with a micrometer head for adjustment. Next, these methods were compared to find out which was the best one. The flexible coupling – micrometer head method was chosen over the compression spring – lead screw method for adjusting the position of the print roller along the Y-axis of the system.

As Table 3 shows, the flexible coupling-micrometer head method was much better in critical design criteria. Based on this decision, the shaft, bearings and flexible coupling have been designed.

Table 2: Pugh Chart

Charudatta Datar

Concept	Weight	Rank		Score	
		Lead Screw	Micrometer Head	Lead Screw	Micrometer Head
Precision (+)	5	1	2	5	10
Cost (-)	2	2	1	4	2
Manufacturability (+)	3	1	2	3	6
Complexity of Design (-)	5	2	1	10	5
Complexity of Assembly (-)	2	2	1	4	2
Usability / Convenience (+)	4	1	2	4	8
Repeatability (+)	4	2	2	8	8
Final Score				38	41

Paolo Baldesi

Concept	Weight	Rank		Score	
		Lead Screw	Micrometer Head	Lead Screw	Micrometer Head
Precision (+)	5	1	2	5	10
Cost (-)	2	2	1	4	2
Manufacturability (+)	3	2	1	6	3
Complexity of Design (-)	5	1	2	5	10
Complexity of Assembly (-)	2	1	2	2	4
Usability / Convenience (+)	4	1	2	4	8
Repeatability (+)	4	2	1	8	4
Final Score				34	41
<b>Average</b>				<b>36</b>	<b>41</b>

### 5.2.3 Shaft and Linear Rotary Bearings Design

Upon designing the magnetic sleeve and the backing plate, keeping in mind the peeling and wrapping processes, next it is necessary to mount the sleeve on the existing machine. This is accomplished by means of a shaft and bearings. The print roller in this system undergoes two primary motions – rotation about its own axis, and translation along its length. The second motion – translation – is mainly to enable adjustment of the print roller position to improve alignment to the order of less than 10 microns. The reader is referred to Paolo Baldesi’s thesis [25] for details about the Precision Positioning System. Hence, in order to fulfill both these motions – rotary as well as linear motion, a linear rotary bearing is chosen. This eliminates the need for two bearings, or one bearing and one bushing.

#### 5.2.4 Linear Rotary Bearing

As stated above, the linear rotary bearing in figure 47 was chosen because it has the ability to account for both, the linear as well as rotary motions of the shaft.

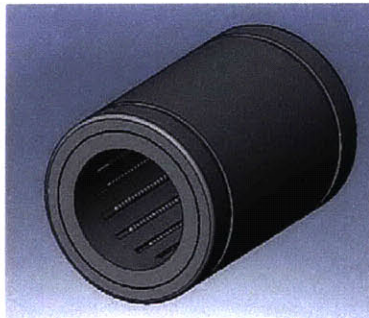


Figure 47: Rotary Linear Bearing [37]

##### 5.2.4.1 Requirement:

Linear rotary bearings allow simultaneous linear and rotary motion.

##### 5.2.4.2 Bearing Selection [26]

Next, the bearing must be designed to withstand loads it will be subjected to, such as weight of the print roller.

Number of bearings required:	2
Total Load:	200 lbs (assuming a jerk)
Maximum speed of rotation:	60 RPM
Shaft Hardening:	RC 55C
Travel Life:	200,000,000”

Note: Travel Life Calculations:

$$\begin{aligned} &= \text{Shaft diameter (inches)} \times 3.1416 \times \text{Revolutions} + \text{Linear Inches Travel} \\ &= 1'' \times 3.1415 \times 60 \times 1,000,000 + 100'' \\ &= \sim 200,000,000'' \end{aligned}$$

### 5.2.4.3 Calculation of Actual Load on Bearing:

Load on each bearing = 200 lbs / 2 = 100 lbs. @ 60 RPM

The actual load on the bearing depends on the shaft hardness and the designed travel life of the bearing. If the shaft is not hardened, it cannot support much of the load, and hence the bearing is subjected to that extra load. The longer the designed travel life of the bearing, the stronger it must be in order to withstand loads for the duration of its life. As a result,

Factored Load Capacity

$$\begin{aligned} &= \text{Load Correction Factor due to Shaft Hardness (K}_h\text{)} \\ &\quad \times \text{Correction Factor for Travel Life (K}_l\text{)} \end{aligned}$$

### Load Correction Factor (K<sub>h</sub>):

For shaft hardness RC 55; from chart below (Figure 48) [27], we obtain K<sub>h</sub> = 0.76

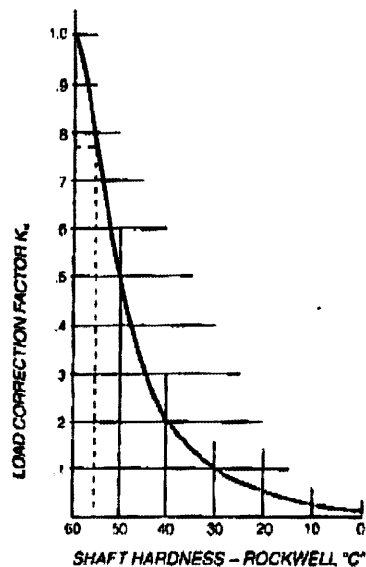


**CHART 4**

Figure 48: Load Correction Factor [27]



**Load Correction Factor (KI)**

Load factor for 200,000,000 inches: from Figure 49 [28], we obtain KI = 0.40

**BEARING SELECTION**

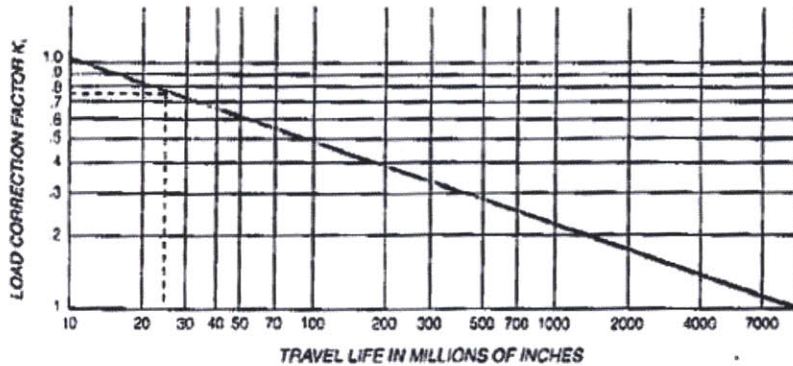


**CHART 3**

Figure 49: Load Factor [28]

Factored load capacity = Load / (Kh x KI) = 100 / (0.76 \* 0.40) = 329 lbs.

From chart below (Table 4) [29], we choose for 329 lbs. @ 60 RPM a Linear Rotary bearing rated at 392 lbs. (LRP-16)

Table 3: Maximum Allowable Loads [29]

**Chart 1 - Maximum Allowable Loads**

Bearing No.	Shaft Dia.	Revolutions per minute											
		Linear Only	50	100	200	300	500	900	1200	1500	1800	2400	3650
LR-6	0.3750	70	61	48	39	33	29	23	21	20	18	17	15
LR-8	0.5000	185	161	128	102	89	76	61	56	52	48	44	39
LR-10	0.6250	283	246	195	156	136	116	93	85	79	74	68	59
LR-12	0.7500	325	283	224	179	156	133	107	98	91	85	78	68
LR-16	1.0000	450	392	311	248	216	185	149	135	126	117	108	95
LR-20	1.2500	600	522	414	330	288	246	198	180	168	156	144	126
LR-24	1.5000	935	813	645	514	449	383	309	281	262	243	224	196
LR-32	2.0000	1340	1166	925	737	643	549	442	402	375	348	322	281
LR-40	2.5000	1830	1592	1263	1018	878	750	604	549	512	475	439	--
LR-48	3.0000	2370	2062	1635	1304	1138	972	782	711	663	616	--	--
LR-64	4.0000	5285	4598	3647	2907	2537	2167	1744	1585	1480	--	--	--

Margin of safety = (392 / 329) - 1 = 19%

Note: This calculation is based on a travel life of 1 million inches.

### 5.2.5 Shaft Design

The magnetic sleeve is mounted on the shaft. And the total run out error of the roller will include any errors in the shaft. Thus the shaft must be precision machined. The shaft must also be compatible with the bearings, etc.

For alignment with the magnetic roller and the web, the shaft must be within the following tolerances:

Diameter: +/- 6 microns

Straightness: +/- 6 microns

The shaft also must take up all the load of the magnetic sleeve, with minimal deformation. The shaft is connected to the magnetic sleeve by means of two setscrews. This basically makes a rigid connection between the shaft and the sleeve, eliminating the possibility of any relative movement between the two. This is very critical to avoid any uncontrolled motion of the print roller.

#### **Design for Linear Rotary Bearings:**

These bearings will be mounted at either end of the length of the shaft. Thus, these ends must meet the following requirements:

Hardness: The linear rotary bearings require that the shaft be case hardened to Rockwell 50-55C

Diameter selection for bearing: Since rotary motion is prominent for the print roller, with a very small amount of linear travel, from the bearing manufacturer's catalog [26], the parts where the bearings would sit on the shaft must have the following tolerances on diameter: 0.9990" to 0.9995"

### 5.2.6 Thrust Bearing

The thrust bearing is press fit into the end of the roller shaft, which comes in contact with the micrometer head (not shown) enabling the X-Axis Registration system. This bearing decouples the rotation of the shaft from the micrometer head, preventing unwanted torques and stresses from developing.

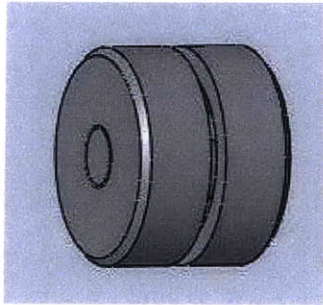


Figure 50: Thrust Bearing [36]

The thrust bearing delivers these functions:

- Provides a stationary surface for the micrometer head to bear upon
- Accounts for the thrust load due to the micrometer head in the X-Axis Registration system.

## 6 Results

### 6.1 New Wrapping Process Results

This section describes the results of using the new magnetic sleeve and the new peeling-wrapping process.

Owing to delays in the procurement of the magnetic sleeve, the backing plate, and other crucial components for the wrapping process, only one experiment was conducted. The peeling-wrapping process was successfully conducted., i.e. no tearing of the PDMS, no deformation or compression of the PDMS due to weight of the roller. Next, a camera was used to capture an image each of two edges of the backing plate on the magnetic sleeve.

Figure 51 illustrates schematically the backing plate wrapped on the magnetic sleeve. The red and the green box show the locations of the image-captures. The two photos were used to compare the precision of wrapping.

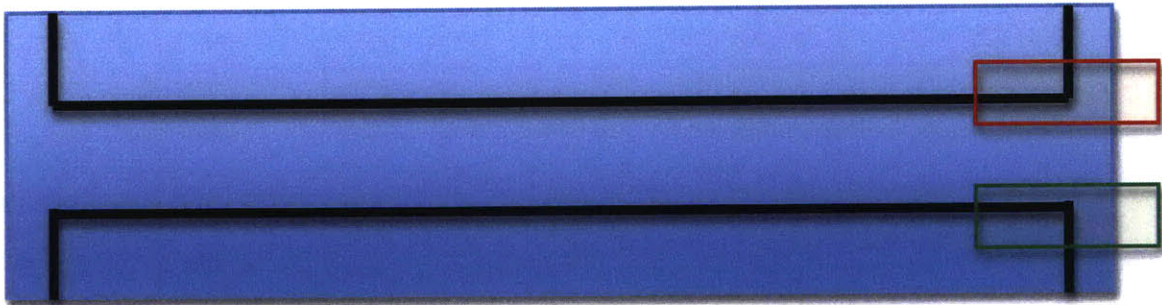


Figure 51: Illustrates backing plate wrapped on the magnetic sleeve. The red and the green frame show locations of photos used for analyzing wrapping precision

These photos are shown in Figures 52 and Figure 53, respectively.

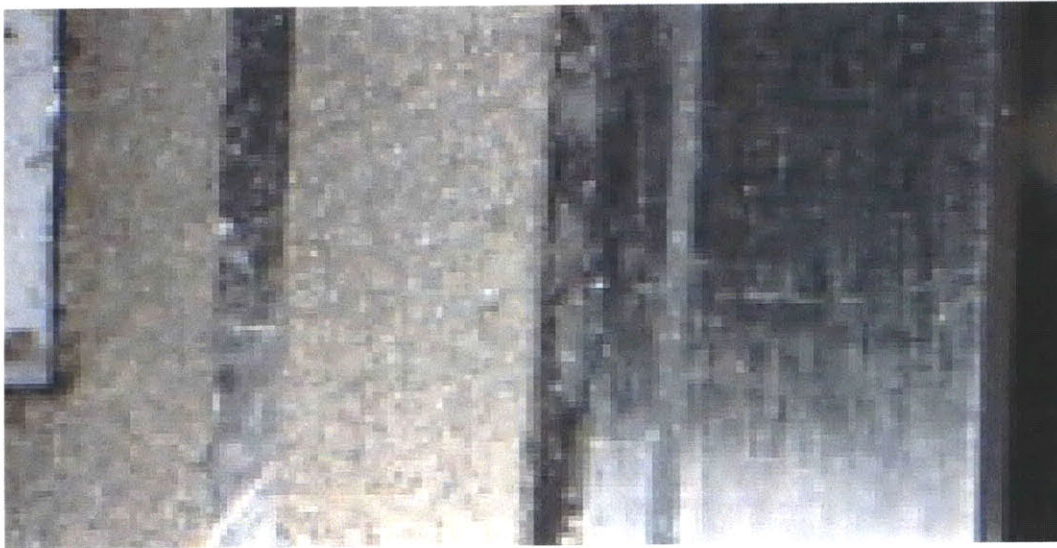


Figure 52: Shows an edge of the backing plate (red frame from Figure 51)

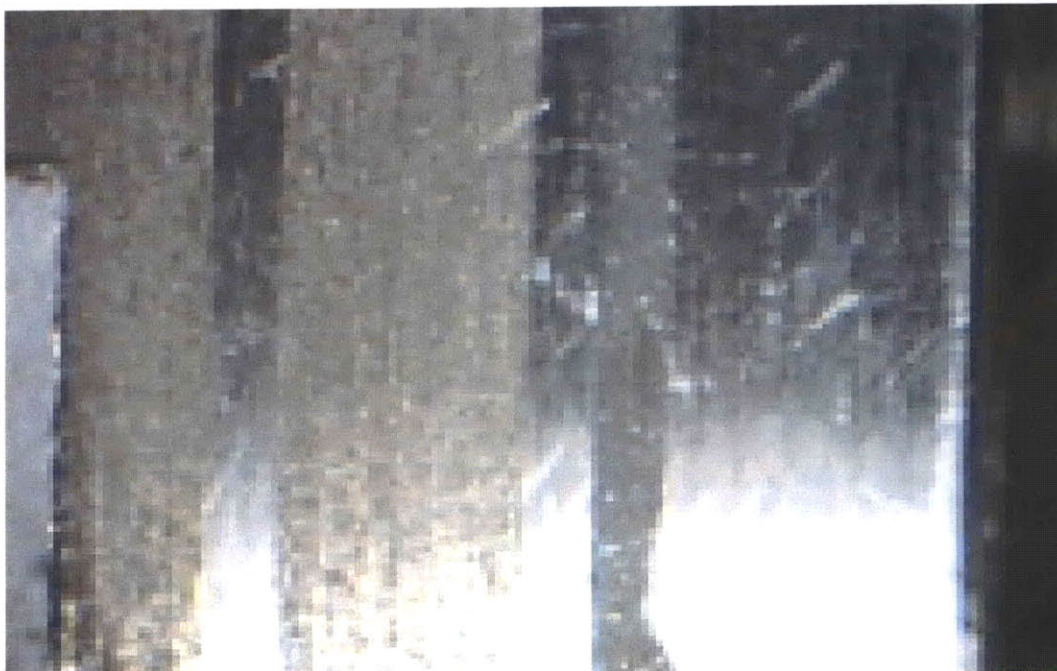


Figure 53: Shows an edge of the backing plate (green frame from Figure 51)

Next, these photos are compared to find the difference between the distances of each edge of the backing plate from that of the magnetic sleeve.

This is illustrated in Figure 54 below.

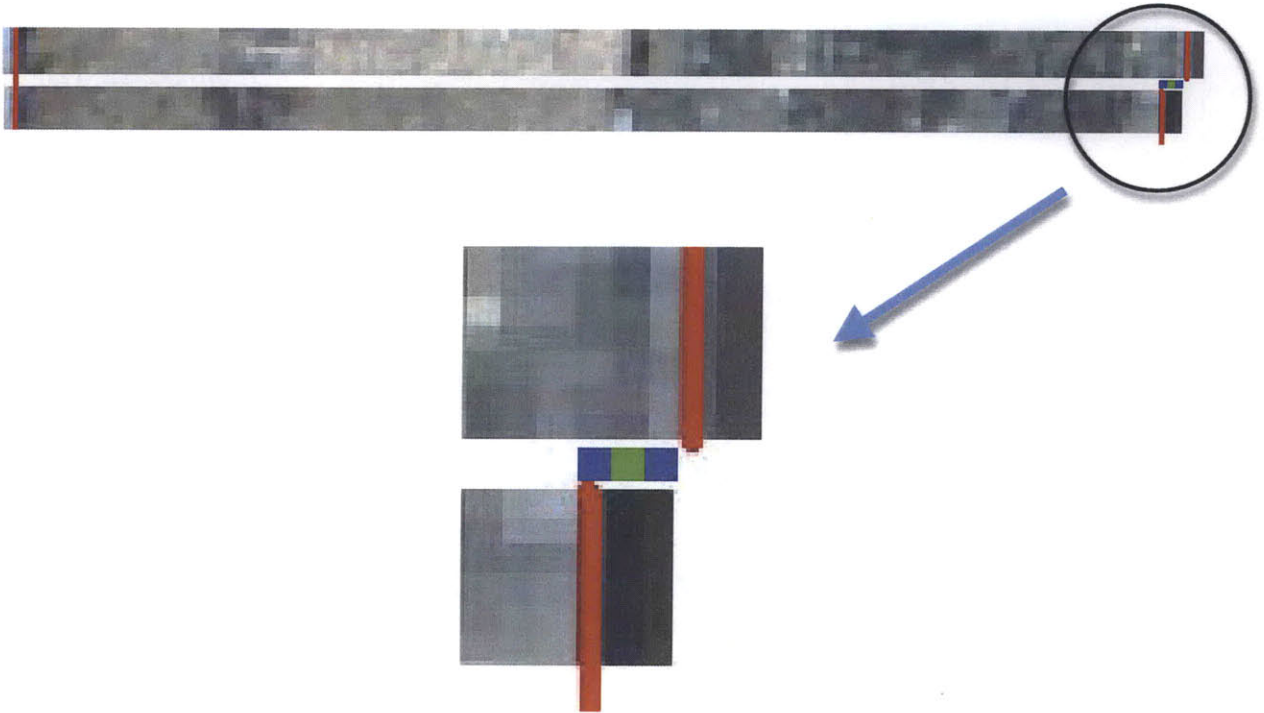


Figure 54: The enlarged photo shows the error, or misalignment during wrapping between the two edges of the backing plate.

In Figure 54, owing to limitations of the photography equipment used, each pixel corresponds to 25 microns. As a result, a resolution better than 25 microns could not be achieved.

Thus, it is evident from figure 54 that the error due to wrapping is 3 pixels, 75 microns. This means that the backing plate is wrapped spirally with one edge misaligned from the other, by a distance of 75 microns.

## **6.2 Assumptions and Discussion:**

This experiment only measures the misalignment at one side of the backing plate. Thus, we assume that all four edges of the backing plate are perfectly square. However, in reality, there will be some amount of error.

Also, we assume that the end faces of the magnetic sleeve are perfectly flat, and parallel to each other. In addition, the magnetic sleeve is assumed to be perfectly straight over its length. However, again, this will not be the case. These parameters were however not measured owing once again to huge delays in the procurement of the print roller.

More measurements, including those of the straightness of each edge of the backing plate, angle between each edge, and perpendicularity between the end faces of the magnetic sleeve would offer better results regarding the misalignment due to wrapping. Overall, this preliminary study indicates that the new wrapping process is capable of high-precision wrapping of the backing plate on the print roller.

## 7 Flat Stamp Casting <sup>[24]</sup>

The following chapter is an excerpt from Yufei Zhu's thesis <sup>[24]</sup>. The section below briefly describes the new stamp fabrication device. For more details, the reader is referred to Yufei Zhu's thesis <sup>[24]</sup>.

### 7.1 Updated Flat Stamp Casting Machine

The new stamp fabrication machine, shown in figure 55, is a modification of the old device described in section 3.1. Improvements of this new design include:

- The wafer can be changed easily and quickly aligned.
- Flatness of stamp is at the level of microns.
- The backing plate is mechanically aligned during stamp fabrication.
- Both vacuum chucks used in this device can be disassembled to remove excess PDMS.
- The machine is capable of maintaining low pressure in the internal area during mold filling.

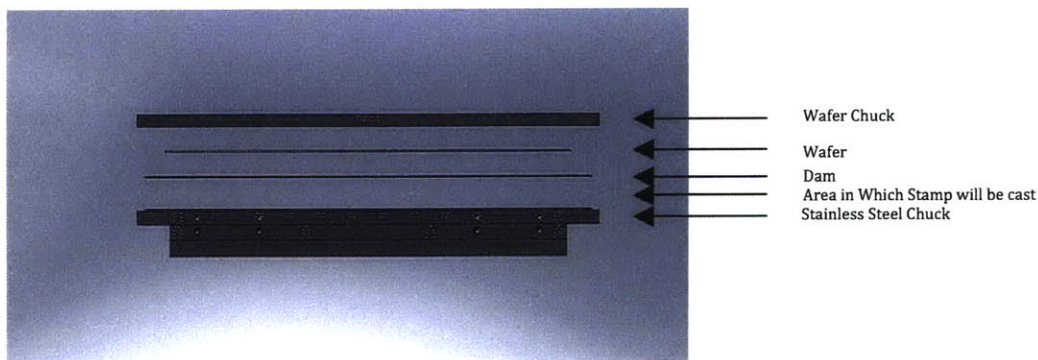


Figure 55: Schematic illustration of the casting machine

### 7.2 Wafer Chuck

The wafer chuck holds the wafer with a vacuum. The wafer chuck (shown in Figure 56) has concentric grooves, to account for PDMS leaks during the casting process. Another circular channel located outside the grooves prevents PDMS from leaking into vacuum area below the wafer. PDMS is injected through a hose.



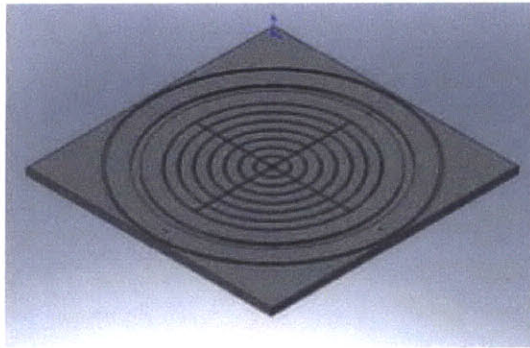


Figure 56: 3D Model of Wafer Chuck for 12" wafer [24].

### 7.3 Stainless Steel Vacuum Chucks

Stainless Steel (SS) Chucks are used to hold the backing plate (SS Sheet) onto which PDMS adheres. For more details about the design of the chucks, please refer Yufei Zhu's thesis<sup>[24]</sup>.

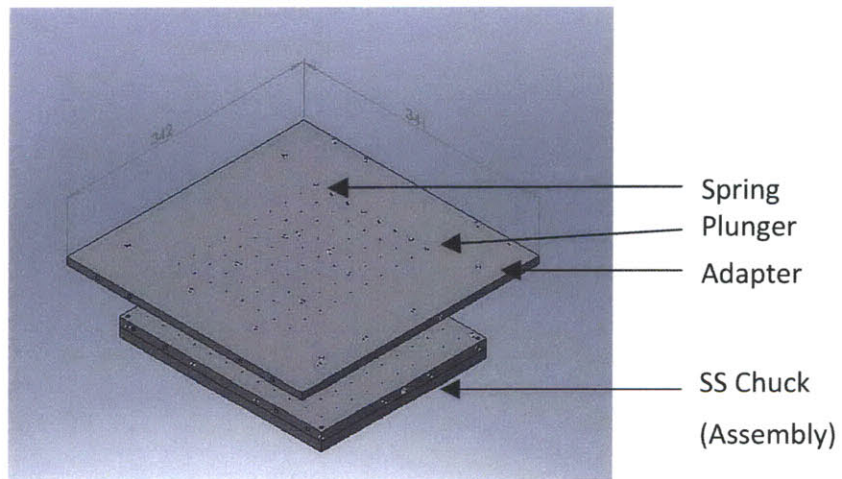
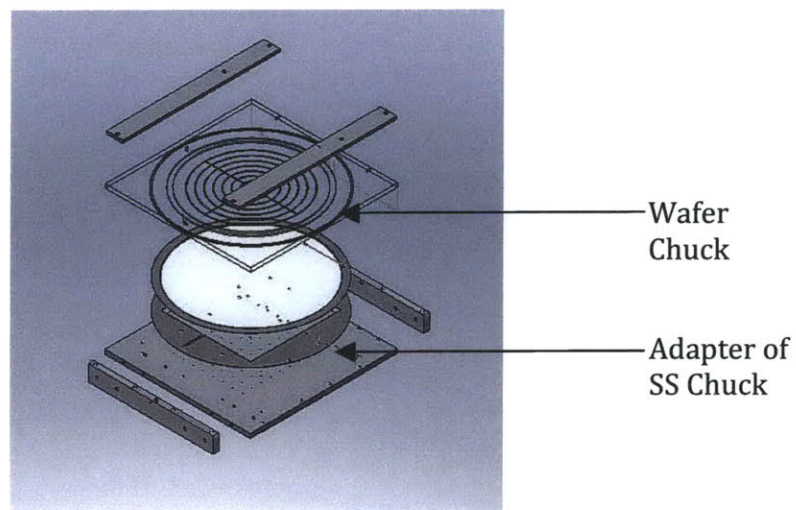


Figure 57: 3D Model of Adapter of SS Chuck for 200mmx200mm Stamp Fabrication [24].

## 7.4 Assembly of Stamp Casting Machine

Assembly of the stamp fabrication device follows the method mentioned in Chapter 3.1. Thin piece of dams are added between the wafer and backing plate to cast different shape of stamp other than circular. In the test conducted at Nano-Terra Inc. we inserted round Teflon with square hole inside for square stamp. The 3D model of the assembled device is shown in Figure 58. The wafer chuck is represented by a wireframe for clear view inside the structure. Two other clamping bars will be added during stamp fabrication. The location of clamping bar is determined by the location of threaded-holes at the sidebar.



**Figure 58:** 3D Model of Assembly for 12" wafer (exploded view). The wafer chuck is represented by a wireframe for a clearer view inside the structure. [24]

## 8 Multi-layer Printing with Updated Roll-to-Roll System [34]

The following chapter is an excerpt from Wenzhuo Yang's thesis [29]. The section below briefly describes the multi layer printing process. For more details, the reader is referred to Wenzhuo Yang's thesis [29].

### 8.1.1 Introduction of Multi-Layer Printing Process

This section briefly describes the multi layer printing process.

The primary target of multi-layer printing is to print the second layer of thiol onto the substrate, on top of the first printed layer. In order to use the updated R2R machine to realize multi-layer printing, continuous feedback of the registration is a must. The basic process of two-layer printing in this project is to print the first layer using the updated R2R machine without any alignment control. Then the substrate is wound back and alignment mark on the substrate is found with the help of a camera to align the web position. After that, the second layer is printed for a certain section of the web, the machine is stopped and the misalignment between two layers is again measured and the rollers adjusted correspondingly using the precision positioning system. As a result, after a few iterative steps, the second layer printing should be aligned with the first layer.

While the above description gives a general idea of the process; some critical parts are detailed below:

1. After the first layer printing, the substrate will not be etched. That means although the substrate has the features that looks like the picture shown in Figure 57, those features are not visible. So, marking the general position of each section of pattern is necessary for the etching in the future. The seam between each section of pattern is due to the area with no stamp on the print roller.

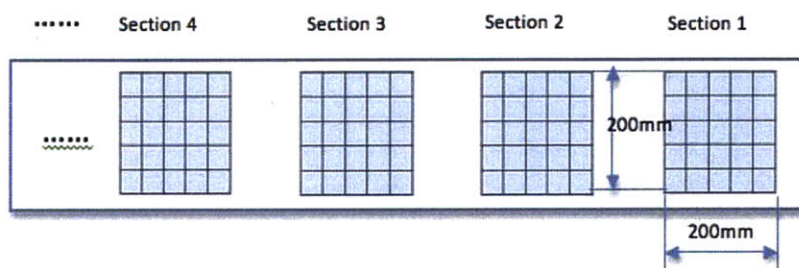


Figure 59: Position of Patterns After First Layer Printing [34]

2. After winding back the printed substrate, the impression roller is translated up a certain distance using micrometer head to disengage it from the print roller. Then, the substrate is wound forward with tension maintained by the torque of the driving motor in the collector module, until the section 1 passes through the print roller (shown in Figure 58). The machine is stopped, keeping the position and tension of the substrate unchanged, and the two cameras are used to find the marks at the edges of section 1. Currently, Nano Terra does not have the capability to make alignment marks on the stamp, so the pixel at the edge of the substrate is used as the mark to align the position, and brushing the etchant onto the substrate, those pixels are developed.

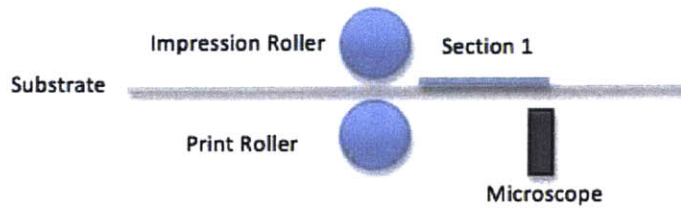


Figure 60: Alignment of the First Layer [34]

3. Adjust two cameras, one at the front of the web and the other at the back, to the position where the “mark pixel” is right at the center of the microscope. (See Figure 59) Then, lock the microscopes on the optical table. Since the 200mmx200mm patterns are periodically printed on the substrate, as soon as the microscope shows the “mark pixel” at the corners, we know that the roller has rotated 360o and the substrate has just floated the length of the perimeter of the print roller, which means the relative position of the print roller and the substrate is traceable.

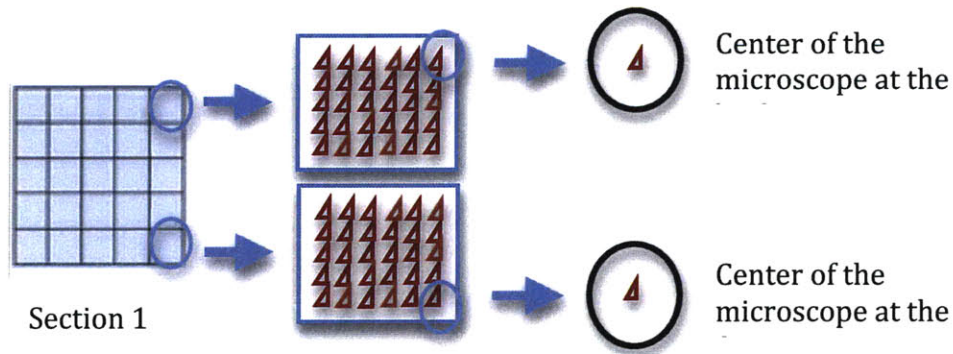


Figure 61: Using Microscope to Align the Position of the Substrate [34]

4. Now, the position of the substrate and the roller is fixed. The impression roller is moved down to the upper surface of the print roller with the substrate in between. We do not want to lose the calibrated position of the substrate by pressing the impression roller onto its surface. So we lock the feeding and collection rollers and let the impression roller stretch the substrate. As soon as the impression roller and the print roller can hold the substrate, the feeding and collection rollers may be loosened.
5. Start the machine to print the second layer on section 2 and then develop the pixels. Align the "mark pixel" right at the center of the camera, to determine the relative position of the print roller and the substrate. Measure the displacement of two layers and adjust print roller to compensate misalignment. For example, in figure 60, the x displacement could be adjusted by rotating the roller in angle of  $X/R$ ; Y displacement could be adjusted by moving the print roller Y units across the printing direction.

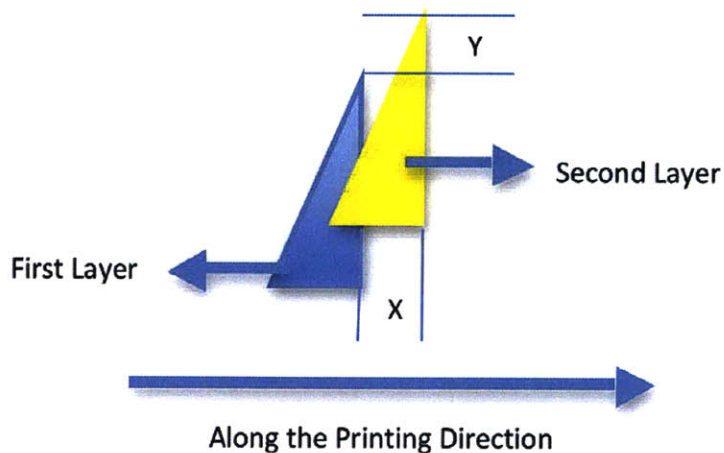


Figure 62: Adjustment of Second Layer printing [34]

6. Ideally, the second layer printing on section 3 should align with the feature on the first layer. If not, re-adjust the print roller and keep printing on section 4. Basically, the machine stops after every printing on each section, align the "mark feature", monitor the overlap of two layers and make adjustment if needed.

## 9 Conclusions and Future Work

### 9.1 Conclusions

The roll-to-roll machine built in 2008 proved the feasibility of single-layer microcontact printing at speeds as high as 400 feet per minute. However, for microcontact printing to be an industry-competitive solution, it was necessary to demonstrate a high-precision multi-layer printing capability. Keeping this goal in mind, several modifications were made to the machine, in order to test this capability of microcontact printing within a limited budget and time frame.

- *Flat Stamp Fabrication Machine:* This machine was designed and built to fabricate a flat PDMS stamp and to overcome poor print quality due to stamps with high thickness variation that were manufactured using the previously used injection molding process.
- This new machine can fabricate stamps with a thickness variation of merely  $\pm 16\mu\text{m}$ .
- *Wrapping System:* Once the flat stamp is cast on a metal backing plate, it is wrapped on the print roller. The wrapping system must minimize stamp distortions during wrapping. The process must also be repeatable, and must guarantee a precision of distortion error within a few microns.
- The new wrapping system makes use of a custom designed magnetic roller and a pin-slot alignment mechanism to achieve high-precision and repeatable wrapping. Preliminary experiment shows that wrapping can be achieved with an absolute misalignment of 75 microns between the backing plate and the roller.
- *Precision Positioning System:* The previous configuration of the roll-to-roll machine did not allow adjustment of the position of the print roller relative to the substrate (web), thus rendering multi-layer printing incapable of achieving high resolution. Thus, a five-axis high-resolution flexure-based system to control the position of the print roller was designed and calibrated to enable an open-loop control to help achieve good quality multi-layer printing. Using this system, the print roller can be positioned and oriented with high repeatability,  $2.5\mu\text{m}$  accuracy, and  $2.5\mu\text{m}$  resolution. Calibration of the precision positioning showed that the five axes are coupled, and in the worst case, this coupling is 8%.
- *Impression Roller:* The impression roller is located above the print roller. The vertical motion of the impression roller was not repeatable, resulting in lack

of control of the final print quality, due to variable pressure. Thus, a new shaft, plate, and precision linear bearings, were used to improve repeatability.

- *Multi-Layer Printing Experiments:* Implementing all of the above improvements, multi-layer experiments were conducted, which revealed that the deformation of the printed output was limited to an average of 3.8%. In addition, a  $\pm 75$  micron misalignment was achieved between two-layers.

## 9.2 Future Work

The above results are based on preliminary experimentation. Also, given the limited time frame and budget, certain components could not be improved, or introduced. Following is the list of improvements we believe will deliver even better results as far as multi-layer printing is concerned:

- *Stamp Fabrication:* Currently, the positioning of the backing plate in the flat stamp machine is not high precision, introducing significant uncertainty in the location of the stamp on the backing plate. A better mechanical positioning system, preferably replacing spring plungers with precision dowel pins, should be used.
- *Wrapping System:* The magnetic print roller is considerably heavy. The current wrapping process is entirely manual. The process could benefit from automation. Automation could also prevent the possibility of accidental damage to holes on the backing plate.
- *Precision Positioning System:* Displacement of the print roller along any axis is a tedious job, and could be easier if digital ones replaced the vertical micrometer heads. Again, automation is essential and a natural progression to introduce a continuous closed-loop control, which will enable very high-precision multi-layer printing.
- *Impression Roller:* This impression roller currently only establishes correct, uniform contact of the print roller with the web. However, if replaced by another print roller, it could equip the existing machine with the capability to print on both sides of the substrate. However, this requirement will be customer or industry dependent, and consequently may not be immediately pursued.
- *High-Resolution Cameras:* The low-resolution of the existing cameras limits the result of misalignment between two printed layers to  $\pm 75$  micron, thus limiting the achievable resolution of multi layer printing. Replacing these cameras, which

provide feedback of the misalignment between two printed layers, with high-resolution ones will help achieve very high-precision multi layer printing.

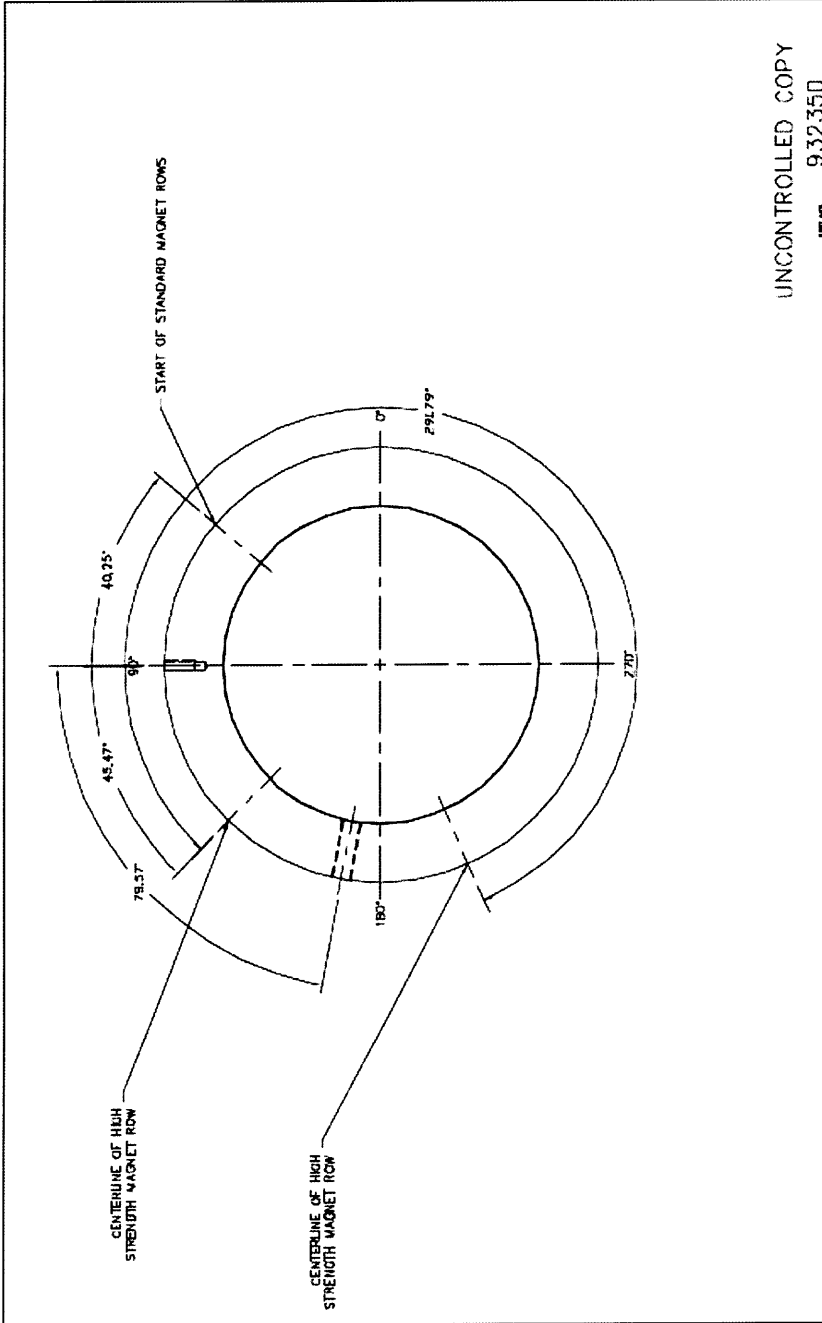
- *Driving Motor:* A stepper motor drives the print roller. A stepper motor is not ideally suited for this kind of operation, which requires a smooth, uninterrupted, step-free rotation of the print roller, and hence a flow of the web. Thus, a stepless motor should be used in place of the stepper motor.
- *Web Control:* One major obstacle in achieving high-resolution multi layer printing with the current configuration is the lack of web control. The position of the web literally defines the result of multi layer printing, and lack of its control severely handicaps any effort to minimize error in multi layer printing. Thus, controlling the web is of utmost importance and should be a top priority.





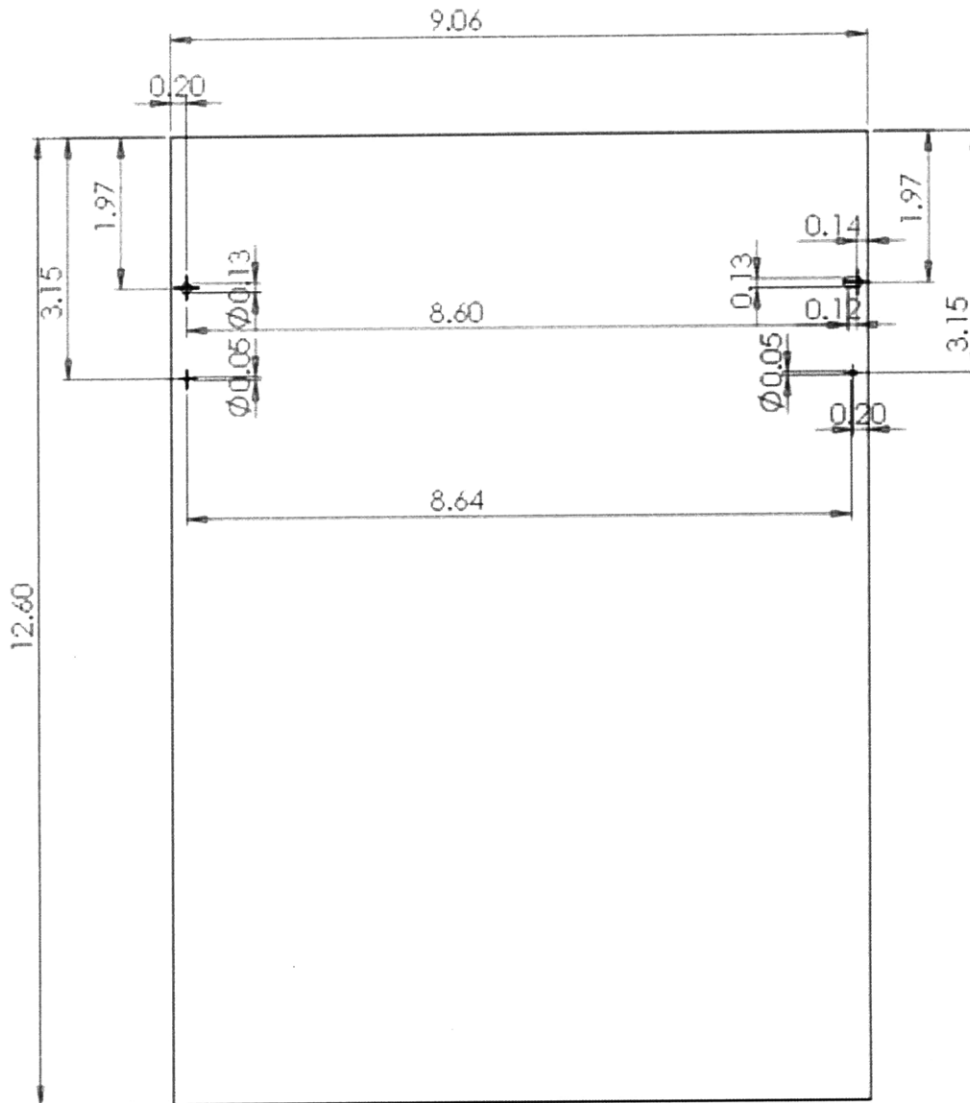


**TITLE: MAGNETIC SLEEVE (SIDE VIEW)**



UNCONTROLLED COPY  
DATE 06 932350

**TITLE: BACKING PLATE**



UNLESS OTHERWISE SPECIFIED:		NAME	DATE	<b>MIT-Nanoterra</b>			
DIMENSIONS ARE IN INCHES		DRAWN	ATS			TITLE: <b>Backing Plate</b>	
TOLERANCES:		CHECKED		SIZE DWG. NO. REV <b>A P114 A</b>			
ANGULAR $\pm .5^\circ$		ENG APPR.				SCALE: 1:2 WEIGHT: SHEET 1 OF 1	
TWO PLACE DECIMAL $\pm .010$		MRG APPR.					
THREE PLACE DECIMAL $\pm .005$		COMMENTS:					
MATERIAL: <b>Spring Steel</b>							
FINISH: <b>TYPE II CLEAR ANODIZE</b>							
DO NOT SCALE DRAWING							

## Bill of Materials, Wrapping System

Item	Description	Qty	MFG	Vendor	Part #
1	MAGNETIC SLEEVE	1	Rotometrics	Rotometrics	W100
2	SHAFT	1	Rotometrics	Rotometrics	W101
3	FLEXIBLE COUPLING	1	RW-America	RW-America	EKL/60/C/14/16
4	LINEAR ROTARY BEARINGS	2	E-LRB	E-LRB	LRP-16
5	BACKING PLATE	1	Rotometrics	Rotometrics	W102
6	THRUST BEARING	1		M-C	7809K351
7	DOWEL PIN	2		M-C	90145A471

## References

- [1] Xia, Y. and Whitesides, G. M., 1998, "Soft Lithography", *Annual Review Mater. Sci.* 1998. 28:153–84
- [2] Nano Terra Inc, <[http://www.nanoterra.com/i/self\\_assembly\\_diagram\\_1.gif](http://www.nanoterra.com/i/self_assembly_diagram_1.gif)>. Accessed 8/1/2008.
- [3] Michel, B. et al., 2000, "Printing Meets Lithography: Soft Approaches to High resolution Patterning", *IBM Journal of Research and Development*, 45(5)
- [4] Stagnaro, A.; "Design and Development of a Roll-to-Roll Machine for Continuous High-Speed Micro-contact Printing"; Massachusetts Institute of Technology, 2008
- [5]. Z.-Q. Gong and K. Komvopoulos. Effect of surface patterning on contact deformation of elastic-plastic layered media. *Journal of Tribology*, 125(1):16-24, 2003.
- [6] K. L. Johnson. *Contact Mechanics*. Cambridge University Press, 1987.
- [7] J. N. Israelachvili. *Intermolecular and surface forces*. Academic Press, 2003.
- [8] K. L. Johnson, K. Kendall, and A. D. Roberts. Surface energy and the contact of elastic solids. *Proceedings of the Royal Society of London Series A, Mathematical and Physical Sciences*, 324(1558):301-313, 1971.
- [9] M. Forster, W. Zhang, A. J. Crosby, and C.M. Stafford. A multilens measurement platform for high-throughput adhesion measurements. *Measurement Science and Technology*, 16(1):81-89, 2005.
- [10] M. K. Chaudhury and G. M. Whitesides. Direct measurement of interfacial interactions between semispherical lenses and flat sheets of poly(dimethylsiloxane) and their chemical derivatives. *Langmuir* 7(5):1013-1025, 1991.
- [11] A. A. Griffith. The phenomena of rupture and flow in solids. *Philosophical Transactions of the Royal Society of London. Series A, Containing Paper of a Mathematical or Physical Character*, 221:163-198, 1921.
- [12] D. Maugis and M Barquins. Fracture mechanics and the adherence of viscoelastic bodies. *Journal of Physics D: Applied Physics*, 11(14):1989-2023, 1978.
- [13] Brian Cotterell, Gordon Williams, John Hutchinson, and Michael Thouless. Announcements of a round robin on the analysis of the peel test. *International Journal of Fracture*, 114(3):9-13, 2002.

- [14] Laser Triangulation Sensors, <[Http:// www.sensorland.com](http://www.sensorland.com)>, Accessed on 08/1/2009
- [15] Interferometry, <[Http://www.wikipedia.com](http://www.wikipedia.com)> accessed on 08/1/2009
- [16] Alexander H. Slocum, Precision Machine Design, Michigan: Society of Manufacturing Engineers Dearborn, 1992
- [17] MTI instrument Inc. <[Http://www.mtiinstruments.com/](http://www.mtiinstruments.com/)>, Optical Fiber, accessed on 08/2009
- [18] Giallorenzi et al., Optical Fiber Sensor Technology, IEEE J. Auantum Electron., Vol. QE-18, No.4 1982,pp.
- [19] Pawley JB (editor) (2006). Handbook of Biological Confocal Microscopy (3rd ed.). Berlin: Springer.
- [20] Khanna,K; "Analysis of the Capabilities of Continuous High-Speed Microcontact Printing"; Massachusetts Institute of Technology, 2008
- [21] Shen, Shawn. "Design and Analysis of High-speed Continuous Micro-Contact Printing". Massachusetts Institute of Technology. August 19, 2008.
- [22] Sriram Krishnan, "On the Manufacture of Very Thin Elastomeric Films by Spin-Coating", Massachusetts Institute of Technology. September 2007
- [23] Con-Focal Microscopy, <[Http://www.wikipedia.com](http://www.wikipedia.com)>, accessed on 08/1/2009
- [24] Zhu, Yufei. "Design and Manufacturing of High Precision Roll-to-Roll Multi-layer Printing Machine- Machine Upgrade". Massachusetts Institute of Technology. August 18, 2009.
- [25] Baldesi, Paolo, "Design and Development of High Precision Five-Axis Positioning System for Roll-to-Roll Multi-Layer Microcontact Printing", Massachusetts Institute of Technology. August 18, 2009.
- [26] Linear Rotary Bearings Inc. <<http://www.e-lrb.com/specifications.htm>>, accessed August 5, 2009
- [27] Linear Rotary Bearings Inc <[http://www.e-lrb.com/images/general/general\\_specifications\\_chart\\_4.jpg](http://www.e-lrb.com/images/general/general_specifications_chart_4.jpg)>, accessed August 5, 2009

[28] Linear Rotary Bearings Inc <[http://www.e-lrb.com/images/general/general\\_specifications\\_chart\\_3.jpg](http://www.e-lrb.com/images/general/general_specifications_chart_3.jpg)>, accessed August 5, 2009

[29] Linear Rotary Bearings Inc <<http://www.e-lrb.com/specifications.htm#Chart%201%20-%20Maximum%20Allowable%20Loads>>, accessed August 5, 2009

[30] R+W America LP <<http://www.rw-america.com/docu-couplings/faq-bellows-elastomer-coupling.php>>, accessed August 7, 2009

[31] Huco Dynatork <[http://www.huco.com/design\\_guide\\_html.asp?page=10](http://www.huco.com/design_guide_html.asp?page=10)>, accessed August 9, 2009

[32] R+W America LP <[http://www.rw-america.com/elastomer\\_couplings/elastomer-insert-properties.php](http://www.rw-america.com/elastomer_couplings/elastomer-insert-properties.php)>, accessed August 9, 2009

[33] University of Rome "La Sapienza", <<http://dma.dma.uniroma1.it/users/broggiato/cdm/roma/no/ecdm/dispense-2008-09/08-FlessionePlastica.pdf>>, accessed August 13, 2009

[34] Yang, Wenzhuo, "Design and Manufacturing of High Precision Roll-to-Roll Multi-layer Printing Machine- Measurement and Experiment", Massachusetts Institute of Technology, August 18, 2009

[35] Miklos, E., June 2, 2009, personal communication

[36] McMaster-Carr, <http://www.mcmaster.com/>, accessed August 1, 2009

[37] Linear Rotary Bearings, <http://e-lrb.com>, accessed August 1, 2009

[38] Rotometrics, <http://www.rotometrics.com/>, accessed August 1, 2009

[39] R + W America LP < [http://www.rw-america.com/elastomer\\_couplings/elastomer-coupling-ekh-t.php#download](http://www.rw-america.com/elastomer_couplings/elastomer-coupling-ekh-t.php#download)>, accessed July 20, 2009